

# Kinetic Study of Aroxyl Radical Scavenging and $\alpha$ -Tocopheroxyl Regeneration Rates of Pyrroloquinolinequinol (PQQH<sub>2</sub>, a Reduced Form of Pyrroloquinolinequinone) in Dimethyl Sulfoxide Solution: Finding of Synergistic Effect on the Reaction Rate due to the Coexistence of $\alpha$ -Tocopherol and PQQH<sub>2</sub>

Aya Ouchi,<sup>\*,†</sup> Kazuto Ikemoto,<sup>‡</sup> Masahiko Nakano,<sup>‡</sup> Shin-ichi Nagaoka,<sup>†</sup> and Kazuo Mukai<sup>\*,†</sup>

<sup>†</sup>Department of Chemistry, Faculty of Science, Ehime University, Matsuyama 790-8577, Japan

<sup>‡</sup>Niigata Research Laboratory, Mitsubishi Gas Chemical Company, Inc., Niigata 950-3112, Japan

**ABSTRACT:** Measurements of aroxyl radical (ArO<sup>•</sup>)-scavenging rate constants ( $k_s^{AOH}$ ) of antioxidants (AOHs: pyrroloquinolinequinol (PQQH<sub>2</sub>),  $\alpha$ -tocopherol ( $\alpha$ -TocH), ubiquinol-10 (UQ<sub>10</sub>H<sub>2</sub>), epicatechin, epigallocatechin, epigallocatechin gallate, and caffeic acid) were performed in dimethyl sulfoxide (DMSO) solution, using stopped-flow spectrophotometry. The  $k_s^{AOH}$  values were measured not only for each AOH but also for the mixtures of two AOHs ((i)  $\alpha$ -TocH and PQQH<sub>2</sub> and (ii)  $\alpha$ -TocH and UQ<sub>10</sub>H<sub>2</sub>). A notable synergistic effect that the  $k_s^{AOH}$  values increase 1.72, 2.42, and 2.50 times for  $\alpha$ -TocH, PQQH<sub>2</sub>, and UQ<sub>10</sub>H<sub>2</sub>, respectively, was observed for the solutions including two kinds of AOHs. Measurements of the regeneration rates of  $\alpha$ -tocopheroxyl radical ( $\alpha$ -Toc<sup>•</sup>) to  $\alpha$ -TocH by PQQH<sub>2</sub> and UQ<sub>10</sub>H<sub>2</sub> were performed in DMSO, using double-mixing stopped-flow spectrophotometry. Second-order rate constants ( $k_r$ ) obtained for PQQH<sub>2</sub> and UQ<sub>10</sub>H<sub>2</sub> were  $1.08 \times 10^5$  and  $3.57 \times 10^4 \text{ M}^{-1} \text{ s}^{-1}$ , respectively, indicating that the  $k_r$  value of PQQH<sub>2</sub> is 3.0 times larger than that of UQ<sub>10</sub>H<sub>2</sub>. It has been clarified that PQQH<sub>2</sub> and UQ<sub>10</sub>H<sub>2</sub> having two HO groups within a molecule may rapidly regenerate two molecules of  $\alpha$ -Toc<sup>•</sup> to  $\alpha$ -TocH. The result indicates that the prooxidant effect of  $\alpha$ -Toc<sup>•</sup> is suppressed by the coexistence of PQQH<sub>2</sub> or UQ<sub>10</sub>H<sub>2</sub>.

**KEYWORDS:** free radicals, pyrroloquinolinequinone, pyrroloquinolinequinol, vitamin E, ubiquinol-10, antioxidant activity, reaction rate, stopped-flow spectrophotometry, coexistence of antioxidants, synergistic effect

## ■ INTRODUCTION

Pyrroloquinolinequinone (PQQ) is a water-soluble quinone compound first identified as a cofactor of alcohol- and glucose-dehydrogenases in bacteria.<sup>1,2</sup> PQQ has been receiving much attention in recent years, owing to its several interesting physiological functions.<sup>3,4</sup> PQQ is regarded to be a nutritionally important growth factor, because PQQ-deficient diets cause impaired growth, immunological defects, and decreased fertility in mice.<sup>5</sup> PQQ is related to mitochondrial biogenesis through cAMP response element-binding protein phosphorylation and increased PGC-1 $\alpha$  expression.<sup>6,7</sup> Moreover, PQQ is related to regeneration of peripheral and central nerves. In *in vitro* experiments, PQQ enhances nerve growth factor, one of the neurotrophic factors responsible for the maintenance and development of peripheral nerves.<sup>8</sup> Regeneration of transected sciatic nerve in an *in vivo* rat model has been demonstrated.<sup>9</sup> It has been suggested that PQQ protects against secondary damage by attenuating inducible nitric oxide synthase (iNOS) expression following a primary physiological injury to spinal cord.<sup>10</sup> A small amount of PQQ has been found not only in microorganisms but also in human and rat organs or tissues, especially in the highest quantity in human milk.<sup>11,12</sup> An additional small amount of PQQ is also found in daily foods and beverages.<sup>13,14</sup>

Previous studies demonstrated that the reduced form of PQQ (PQQH<sub>2</sub> (pyrroloquinolinequinol), see Figure 1) exhibits antioxidative capacity in *in vitro* examinations.<sup>15,16</sup> We found

that PQQNa<sub>2</sub> (disodium salt of PQQ) is easily reduced to PQQH<sub>2</sub>, by reacting PQQNa<sub>2</sub> with glutathione and cysteine in buffer solution (pH 7.4) under nitrogen atmosphere.<sup>17</sup> This result suggests that PQQ exists as a reduced form throughout the cell and plays a role as an antioxidant. In experiments using cultured cells, it was reported that PQQ prevents oxidative stress-induced neuronal death.<sup>18,19</sup> Moreover, marked decreases in ischemia damage are found in *in vivo* models such as cardiovascular or cerebral ischemia models.<sup>20,21</sup> Furthermore, it was reported that PQQ prevents cognitive deficit caused by oxidative stress in rats.<sup>22,23</sup>

Lipid peroxy radical (LOO<sup>•</sup>) and singlet oxygen (<sup>1</sup>O<sub>2</sub>) are well-known as two representative reactive oxygen species generated in biological systems. In previous work, a kinetic study of the aroxyl radical (ArO<sup>•</sup>)-scavenging activity of PQQH<sub>2</sub> and water-soluble antioxidants (AOHs) (such as vitamin C (Vit C), uric acid (UA), cysteine, and glutathione) was performed in 5.0 wt % Triton X-100 micellar solution (pH 7.4) using stopped-flow spectrophotometry (see reaction 1).<sup>17</sup> A stable aroxyl radical (ArO<sup>•</sup>) (2,6-di-*tert*-butyl-4-(4'-methoxyphenyl)phenoxy) (see Figure 1) was used as a model of LOO<sup>•</sup> radical, as described in previous studies.<sup>24–26</sup>

**Received:** September 10, 2013

**Revised:** October 30, 2013

**Accepted:** October 31, 2013

**Published:** October 31, 2013

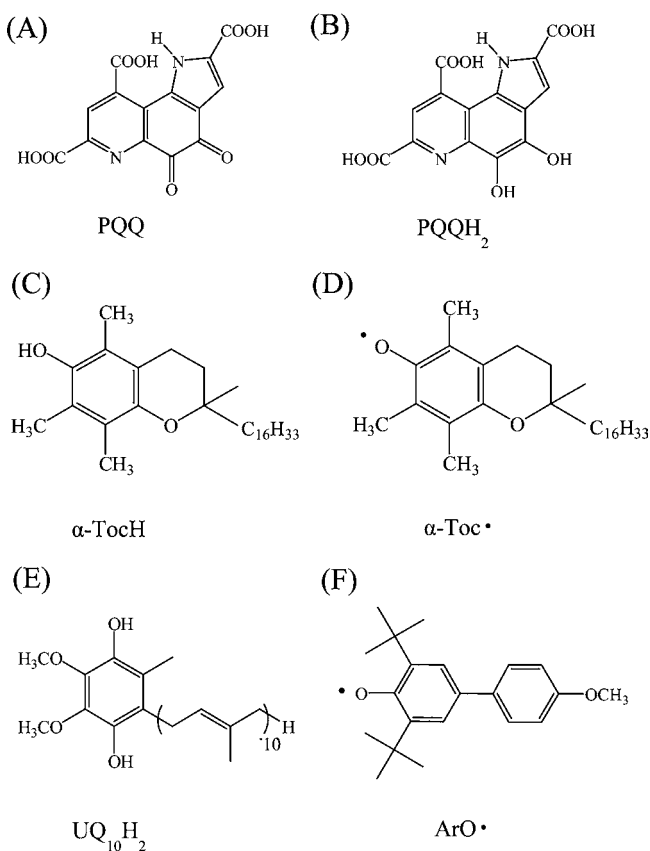
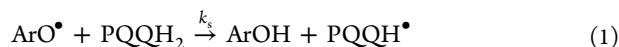


**Figure 1.** Molecular structures of pyrroloquinolinequinone (PQQ), pyrroloquinolinequinol (PQQH<sub>2</sub>), α-tocopherol (α-TocH), α-tocopheroxyl radical (α-Toc•), ubiquinol-10 (UQ<sub>10</sub>H<sub>2</sub>), and aroxyl radical (ArO•).

The second-order rate constants ( $k_s$ ) for the reaction of ArO• with PQQH<sub>2</sub> was found to be 7.4 times larger than that of Vit C, which is well-known as the most active water-soluble AOH.



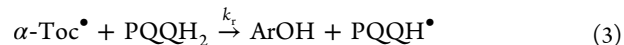
Furthermore, a kinetic study of the quenching reaction of <sup>1</sup>O<sub>2</sub> with PQQH<sub>2</sub>, PQQNa<sub>2</sub>, and seven natural AOHs (Vit C, UA, epicatechin (EC), epigallocatechin (EGC), α-tocopherol (α-TocH), ubiquinol-10 (UQ<sub>10</sub>H<sub>2</sub>), and β-carotene (β-Car)) (reaction 2) has been performed in 5.0 wt % Triton X-100 micellar solution (pH 7.4), indicating that PQQH<sub>2</sub> shows high <sup>1</sup>O<sub>2</sub>-quenching activity.<sup>27</sup>



These results suggest that PQQH<sub>2</sub> may contribute to the protection of oxidative damage in biological systems by scavenging free radicals and quenching <sup>1</sup>O<sub>2</sub>.

In the present study, measurements of the second-order rate constant ( $k_s$ ) were performed for reaction of ArO• radical with PQQH<sub>2</sub> and representative lipid- and water-soluble AOHs (such as α-TocH, UQ<sub>10</sub>H<sub>2</sub>, three catechins, and caffeic acid (CA); reaction 1) in dimethyl sulfoxide (DMSO) solution at 25 °C using stopped-flow spectrophotometry. Measurements of the  $k_s$  value were also performed for the solutions including two kinds of AOHs ((i) α-TocH and PQQH<sub>2</sub> and (ii) α-TocH and UQ<sub>10</sub>H<sub>2</sub>), in order to investigate the synergistic effect of AOHs on the ArO• radical-scavenging rate. Furthermore, measurements of the rate constant ( $k_t$ ) for reactions of α-tocopheroxyl

(α-Toc•) radical with PQQH<sub>2</sub> and UQ<sub>10</sub>H<sub>2</sub> (reaction 3) were performed in DMSO solution using double-mixing stopped-flow spectrophotometry.



## MATERIALS AND METHODS

**Materials.** A brown colored powder sample of PQQH<sub>2</sub> was supplied from Mitsubishi Gas Chemical Company, Inc. α-Tocopherol (α-TocH) and ubiquinone-10 (UQ<sub>10</sub>) were kindly supplied from Eisai Co. Ltd. and Kaneka Co. Ltd., Japan, respectively. Epicatechin (EC), epigallocatechin (EGC), and epigallocatechin gallate (EGCG) were kindly supplied from Mitsui Norin Co., Ltd., Japan. Caffeic acid (CA) was obtained from Nacalai Tesque, Japan. Ubiquinol-10 (UQ<sub>10</sub>H<sub>2</sub>) was prepared by the reduction of UQ<sub>10</sub> with sodium hydrosulfite in *n*-hexane under a nitrogen atmosphere.<sup>26</sup> ArO• radical was prepared according to the method of Rieker and Scheffler.<sup>28</sup>

**Methods.** Measurement of the second-order rate constant ( $k_s$ ) for the reaction of ArO• with AOH (reaction 1) was performed with a Unisoku single-mixing stopped-flow spectrophotometer (model RSP-1000) by mixing equal volumes of DMSO solutions of ArO• and AOH under nitrogen atmosphere.<sup>17,24–26</sup> The  $k_t$  values of PQQH<sub>2</sub> and UQ<sub>10</sub>H<sub>2</sub> (reaction 3) were measured with a Unisoku double-mixing stopped-flow spectrophotometer (model RSP-1000-03F). The details of measurements were reported in previous studies.<sup>29</sup> All the measurements were performed at 25.0 ± 0.5 °C. Experimental errors in the rate constants ( $k_s$  and  $k_t$ ) were estimated to be about 5% in DMSO solution. Ethanol had been generally used for measurements of the  $k_s$  and  $k_t$  values of AOHs in previous studies. However, DMSO was used in the present study, because the solubility of PQQH<sub>2</sub> is low in ethanol. PQQH<sub>2</sub> is stable in DMSO solution.

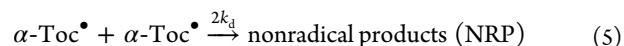
## RESULTS

**Measurements of the Aroxyl Radical Scavenging Rates ( $k_s$  (alone)) for PQQH<sub>2</sub> and Six Natural Antioxidants in DMSO Solution.** Measurement of the rate constant ( $k_s$ ) for reaction of ArO• radical with α-TocH was performed in DMSO solution (reaction 1). By reacting α-TocH with ArO• radical, the absorbance at 380 and 587 nm of the ArO• decreases, and the absorbance at 428 nm of α-Toc• radical increases, as shown in Figure 2A. The scavenging rate of ArO• was measured by following the decrease in absorbance at 380 or 587 nm of the ArO• radical, as shown in Figure 2B.<sup>17,24–26</sup> The pseudo-first-order rate constants ( $k_{\text{obsd}}$ ) at 380 or 587 nm were linearly dependent on the concentration of α-TocH ([α-TocH]), and thus, the rate equation is expressed as

$$-d[\text{ArO}^\bullet]/dt = k_{\text{obsd}}[\text{ArO}^\bullet] = k_s[\alpha\text{-TocH}][\text{ArO}^\bullet] \quad (4)$$

where  $k_s$  is the second-order rate constant for oxidation of α-TocH by ArO• radical. The rate constant ( $k_s$ ) was obtained by plotting  $k_{\text{obsd}}$  against [α-TocH], as shown in Figure 2C. The  $k_s^{\alpha\text{-TocH}}$  (alone) value obtained is  $7.02 \times 10^2 \text{ M}^{-1} \text{ s}^{-1}$  (see Table 1), where “ $k_s^{\alpha\text{-TocH}}$  (alone)” means the ArO•-radical scavenging rate constants obtained in solution including only one component of AOH.

As described above, by reacting α-TocH with ArO• in DMSO, α-Toc• is produced rapidly. α-Toc• is unstable at 25.0 °C; its absorption peak decreases gradually after passing through the maximum and disappears by a bimolecular reaction (reaction 5; see Figure 2D).<sup>30</sup>



As shown in Figure 2D, the maximum absorbance of α-Toc• observed at  $t_{\text{max}}$  increases with increasing [α-TocH] and

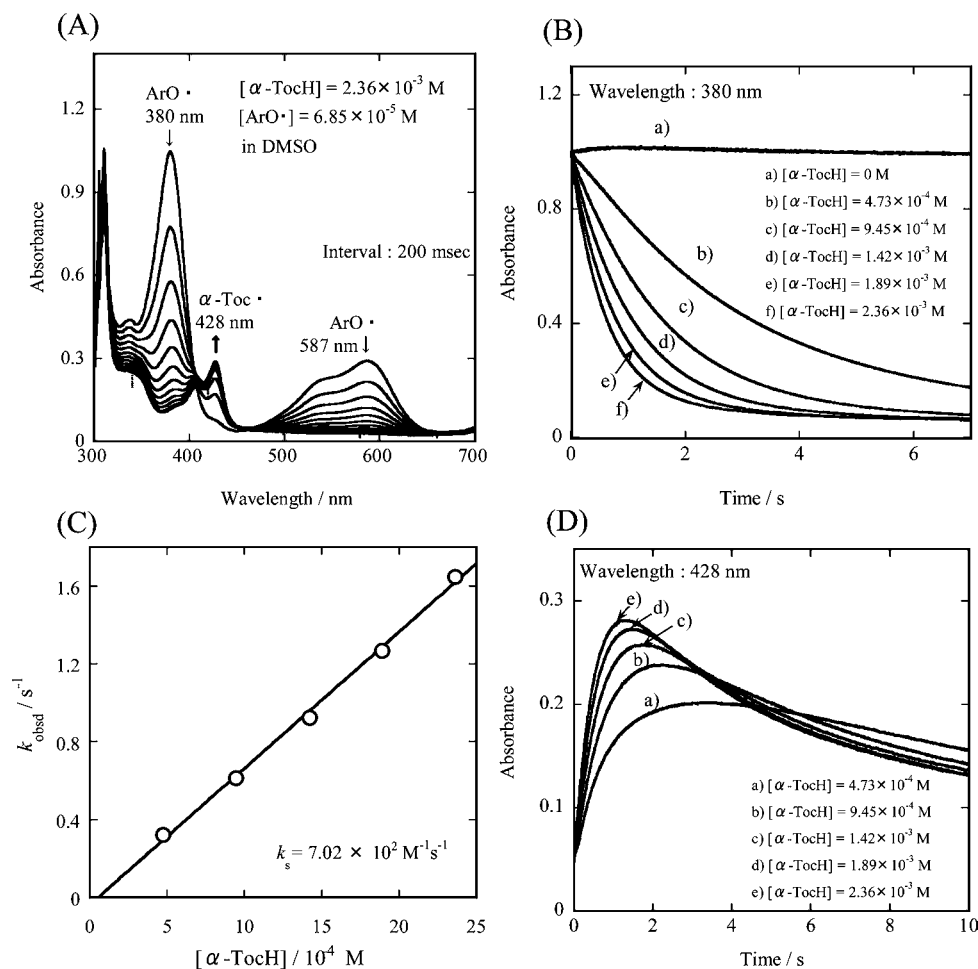


**Figure 2.** (A) Change in electronic absorption spectra of  $\text{ArO}^\bullet$  and  $\alpha\text{-Toc}^\bullet$  radicals during reaction of  $\text{ArO}^\bullet$  with  $\alpha\text{-TocH}$  in DMSO solution at 25.0 °C. Initial concentration is  $[\text{ArO}^\bullet] = 6.85 \times 10^{-5} \text{ M}$  and  $[\alpha\text{-TocH}] = 2.36 \times 10^{-3} \text{ M}$ . Spectra were recorded at 200 ms intervals. Arrow indicates a decrease ( $\text{ArO}^\bullet$ ) and an increase ( $\alpha\text{-Toc}^\bullet$ ) in absorbance with time. Time dependences of the absorbance of (B)  $\text{ArO}^\bullet$  radical (at 380 nm) and (D)  $\alpha\text{-Toc}^\bullet$  radical (at 428 nm) in solutions including six and five different concentrations of  $\alpha\text{-TocH}$  at 25.0 °C, respectively. (C) Pseudo-first-order rate constant ( $k_{\text{obsd}}$ ) versus  $[\alpha\text{-TocH}]$  plot.

**Table 1.** Second-Order Rate Constants ( $k_s^{\text{AOH}}$  (alone)) for Reaction 1 of  $\text{ArO}^\bullet$  Radical with Seven Kinds of Antioxidants (AOHs), Relative Rate Constants ( $k_s^{\text{AOH}}$  (alone)/ $k_s^{\alpha\text{-TocH}}$  (alone)), and Second-Order Rate Constants ( $k_r^{\text{AOH}}$ ) for Reaction 3 of  $\alpha\text{-Toc}^\bullet$  Radical with Ubiquinol-10 and  $\text{PQQH}_2$  in DMSO Solution at 25.0 °C

antioxidant	$k_s^{\text{AOH}}$ (alone), <sup>a</sup> $\text{M}^{-1} \text{s}^{-1}$	avg $k_s^{\text{AOH}}$ (alone), $\text{M}^{-1} \text{s}^{-1}$ <sup>b</sup>	$k_s^{\text{AOH}}$ (alone)/ $k_s^{\alpha\text{-TocH}}$ (alone)	$k_r^{\text{AOH}}$ , <sup>a</sup> $\text{M}^{-1} \text{s}^{-1}$
$\alpha\text{-TocH}$	$(7.31 \pm 0.21) \times 10^2$ $(7.02 \pm 0.22) \times 10^2$ $(7.47 \pm 0.08) \times 10^2$ $(7.55 \pm 0.08) \times 10^2$ $(7.36 \pm 0.25) \times 10^2$	$7.34 \times 10^2$	1.00	
$\text{UQ}_{10}\text{H}_2$	$(1.16 \pm 0.01) \times 10^3$ $(1.27 \pm 0.02) \times 10^3$ $(1.25 \pm 0.02) \times 10^3$	$1.23 \times 10^3$	1.68	$(3.57 \pm 0.13) \times 10^4$
$\text{PQQH}_2$	$(2.63 \pm 0.04) \times 10^2$ $(2.54 \pm 0.03) \times 10^2$ $(2.43 \pm 0.04) \times 10^2$ $(2.48 \pm 0.06) \times 10^2$	$2.52 \times 10^2$	0.343	$(1.08 \pm 0.02) \times 10^5$
EGCG	$(1.58 \pm 0.07) \times 10^2$ $(1.52 \pm 0.08) \times 10^2$	$1.55 \times 10^2$	0.211	
EGC	$(1.22 \pm 0.03) \times 10^2$		0.166	
EC	$(1.86 \pm 0.06) \times 10$		0.0253	
CA	$(1.09 \pm 0.04) \times 10$		0.0149	

<sup>a</sup>Given as value  $\pm$  standard deviation. <sup>b</sup>Avg denotes the average value.

approaches a constant value, because at high  $[\alpha\text{-TocH}]$   $\alpha\text{-Toc}^\bullet$  appears rapidly and the decay of  $\alpha\text{-Toc}^\bullet$  is very small and negligible. Therefore, we can estimate the  $\varepsilon$  value of  $\alpha\text{-Toc}^\bullet$  radical at  $\lambda_{\text{max}} = 428$  nm by assuming that  $[\alpha\text{-Toc}^\bullet]$  at  $t_{\text{max}}$  equals  $[\text{ArO}^\bullet]$  at  $t = 0$  s and using Lambert–Beer's equation (absorbance (of  $\alpha\text{-Toc}^\bullet$  at  $t_{\text{max}} = \varepsilon \times [\text{ArO}^\bullet]_{t=0}$ ), as reported in a previous study.<sup>30</sup> The  $\varepsilon$  value of  $\alpha\text{-Toc}^\bullet$  radical obtained was  $3930 \text{ M}^{-1} \text{ cm}^{-1}$  in DMSO solution.

Similarly, by reacting  $\text{UQ}_{10}\text{H}_2$  with  $\text{ArO}^\bullet$  radical, the absorbance at 380 nm of  $\text{ArO}^\bullet$  decreases rapidly, as shown in Figure 3A. The rate constant ( $k_s^{\text{UQ}_{10}\text{H}_2}$  (alone)) was obtained by

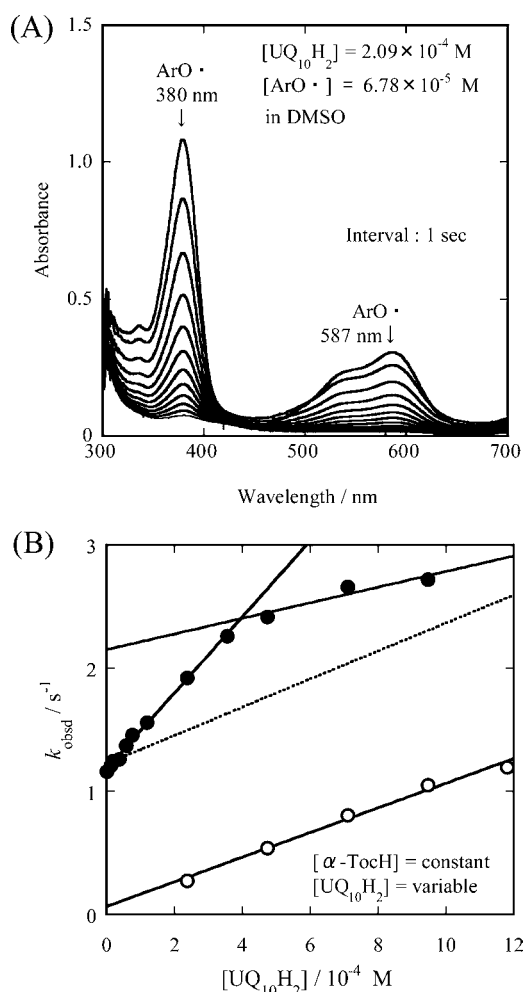


**Figure 3.** (A) Change in electronic absorption spectrum of  $\text{ArO}^\bullet$  radical during reaction of  $\text{ArO}^\bullet$  with  $\text{UQ}_{10}\text{H}_2$  in DMSO at  $25.0$  °C. Initial concentration is  $[\text{ArO}^\bullet] = 6.78 \times 10^{-5} \text{ M}$  and  $[\text{UQ}_{10}\text{H}_2] = 2.09 \times 10^{-4} \text{ M}$ . Absorption of  $\text{UQ}_{10}\text{H}^\bullet$  was not observed. (B) Plots of  $k_{\text{obsd}}$  versus  $[\text{UQ}_{10}\text{H}_2]$  for reactions of  $\text{ArO}^\bullet$  radical with (i)  $\text{UQ}_{10}\text{H}_2$  only (O) and (ii) mixture of  $\alpha\text{-TocH}$  and  $\text{UQ}_{10}\text{H}_2$  (●) (see Table 2B). Dotted line shows the plots for which any synergistic effect is absent between  $\alpha\text{-TocH}$  and  $\text{UQ}_{10}\text{H}_2$ .

plotting  $k_{\text{obsd}}$  against  $[\text{UQ}_{10}\text{H}_2]$  (see Figure 3B). As shown in Figure 3A, we could not observe the absorption spectrum of  $\text{UQ}_{10}\text{H}^\bullet$  radical because of its instability.<sup>31</sup> By reaction of  $\text{PQQH}_2$  with  $\text{ArO}^\bullet$ , the absorbance at 587 nm of the  $\text{ArO}^\bullet$  decreases rapidly, as shown in Figure 4A. Measurement of the decay curve was performed at 610 nm, because strong absorption of  $\text{PQQH}_2$  overlaps that of  $\text{ArO}^\bullet$  at the wavelength region of 380–580 nm (see Figure 4A). The baseline

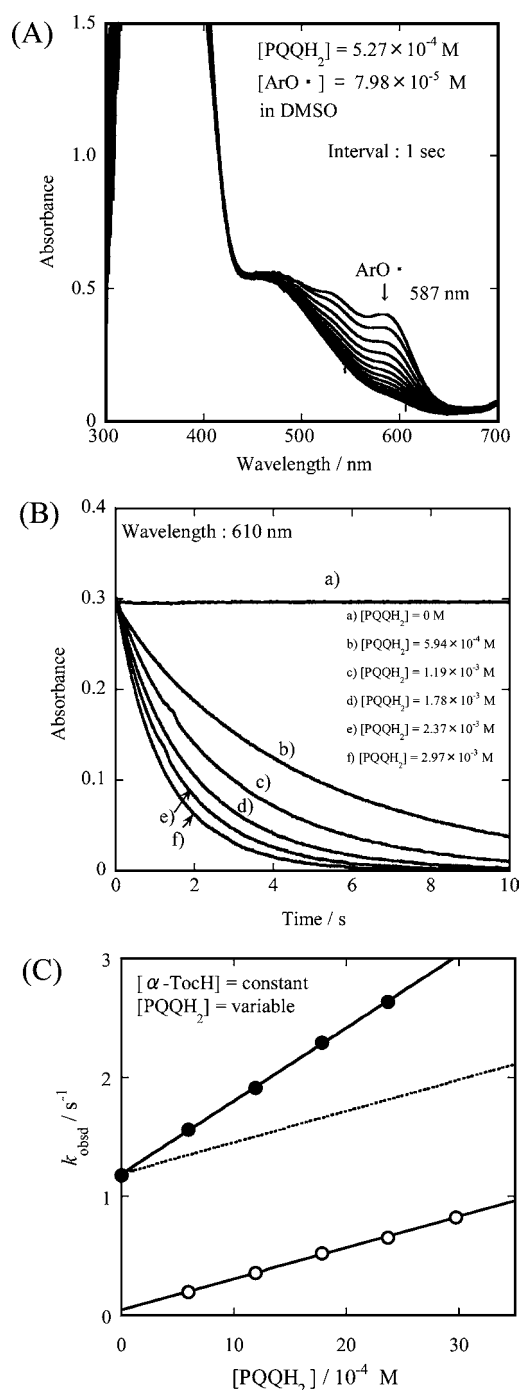


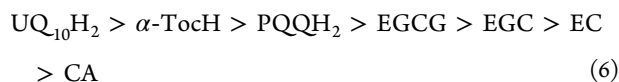
**Figure 4.** (A) Change in electronic absorption spectrum of  $\text{ArO}^\bullet$  radical during reaction of  $\text{ArO}^\bullet$  with  $\text{PQQH}_2$  in DMSO at  $25.0$  °C.  $[\text{ArO}^\bullet] = 7.98 \times 10^{-5} \text{ M}$  and  $[\text{PQQH}_2] = 5.27 \times 10^{-4} \text{ M}$ . (B) Time dependences of the absorbance of  $\text{ArO}^\bullet$  radical at 610 nm in DMSO solutions including six different concentrations of  $\text{PQQH}_2$ , where the correction of baseline due to  $\text{PQQH}_2$  was performed (see text). (C) Plots of  $k_{\text{obsd}}$  versus  $[\text{PQQH}_2]$  for reactions of  $\text{ArO}^\bullet$  radical with (i)  $\text{PQQH}_2$  only (O) and (ii) mixture of  $\alpha\text{-TocH}$  and  $\text{PQQH}_2$  (●) (see Table 2B). Dotted line shows the plots for which any synergistic effect is absent between  $\alpha\text{-TocH}$  and  $\text{PQQH}_2$ .

corrections were performed by using the value of  $\varepsilon = 31.7 \text{ M}^{-1} \text{ cm}^{-1}$  at 610 nm of  $\text{PQQH}_2$  in DMSO, as shown in Figure 4B. The rate constant ( $k_s^{\text{PQQH}_2}$  (alone)) was obtained by plotting  $k_{\text{obsd}}$  against  $[\text{PQQH}_2]$  (see Figure 4C).



Measurements of the  $k_s^{\text{AOH}}$  (alone) values were repeated 3–5 times for every  $\alpha$ -TocH,  $\text{UQ}_{10}\text{H}_2$ , and  $\text{PQQH}_2$  to obtain reliable  $k_s^{\text{AOH}}$  (alone) values. Each  $k_s^{\text{AOH}}$  (alone) value and average  $k_s^{\text{AOH}}$  (alone) values (showing experimental errors) obtained are summarized in Table 1. The  $k_s^{\text{AOH}}$  (alone) values of  $\text{UQ}_{10}\text{H}_2$  and  $\text{PQQH}_2$  are 1.68 and 0.343 times as large as that of  $\alpha$ -TocH, respectively.

Furthermore, the  $k_s^{\text{AOH}}$  (alone) values were measured for four kinds of well-known phenolic AOHs (EC, EGC, EGCG, and CA) to compare the  $k_s^{\text{AOH}}$  (alone) values with that of  $\text{PQQH}_2$ . The results obtained are listed in Table 1, together with those of  $\alpha$ -TocH,  $\text{UQ}_{10}\text{H}_2$ , and  $\text{PQQH}_2$ . The  $k_s^{\text{AOH}}$  (alone) values obtained decreased in the order of eq 6.



The  $k_s^{\text{AOH}}$  (alone) value of  $\text{PQQH}_2$  was greater than those of hydrophilic AOHs (EGCG, EGC, EC, and CA) in DMSO solution. However, it was less than those of lipophilic AOHs ( $\text{UQ}_{10}\text{H}_2$  and  $\alpha$ -TocH).

**Measurements of the Regeneration Rates ( $k_r$ ) of  $\alpha$ -Tocopherol by  $\text{PQQH}_2$  and Ubiquinol-10 in DMSO Solution.** As described in the Methods section, measurement of the  $k_r$  value for reaction of  $\alpha\text{-Toc}^\bullet$  radical with  $\text{UQ}_{10}\text{H}_2$  (reaction 3) was performed in DMSO solution, using a double-mixing stopped-flow spectrophotometer.<sup>29</sup>  $\alpha\text{-Toc}^\bullet$  radical was prepared by the first-mixing of equal volumes of  $\alpha$ -TocH (cell A) and  $\text{ArO}^\bullet$  (cell B) solutions (reaction 1), and after 2 s the second-mixing of equal volumes of  $\alpha\text{-Toc}^\bullet$  solution and  $\text{UQ}_{10}\text{H}_2$  solution (cell C) (reaction 3) was made. The typical concentrations in cells A and B are  $7.24 \times 10^{-3}$  and  $5.14 \times 10^{-4}$  M, respectively. The decay curves of the absorbance of  $\alpha\text{-Toc}^\bullet$  at 428 nm in DMSO are shown in Figure 5A, indicating that the decay rates increase with increasing  $[\text{UQ}_{10}\text{H}_2]$ .

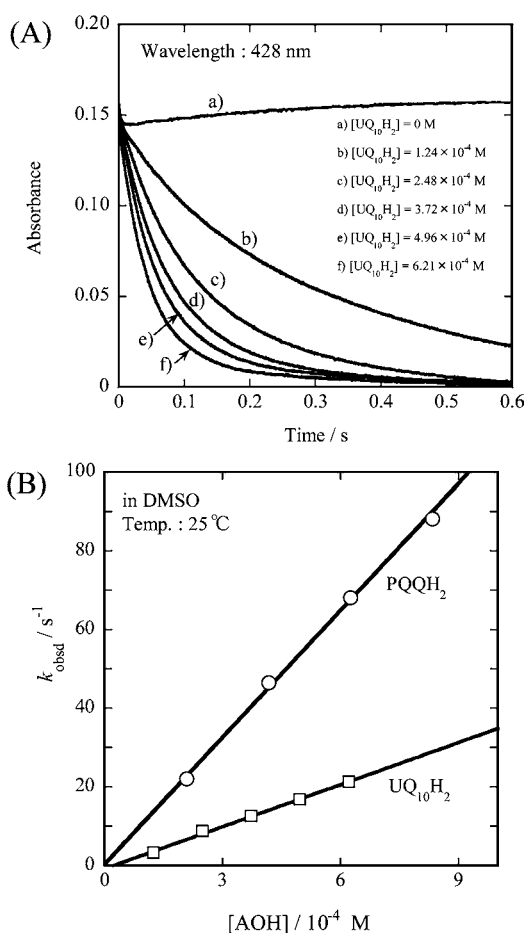
The pseudo first-order rate constants ( $k_{\text{obsd}}$ ) observed at 428 nm were linearly dependent on  $[\text{UQ}_{10}\text{H}_2]$ , and thus, the rate equation is expressed as follows:

$$-d[\alpha\text{-Toc}^\bullet]/dt = k_{\text{obsd}}[\alpha\text{-Toc}^\bullet] = k_r[\text{UQ}_{10}\text{H}_2][\alpha\text{-Toc}^\bullet] \quad (7)$$

The  $k_r$  value was obtained by plotting  $k_{\text{obsd}}$  against  $[\text{UQ}_{10}\text{H}_2]$ , as shown in Figure 5B.

Similar measurements were performed for the reaction of  $\alpha\text{-Toc}^\bullet$  with  $\text{PQQH}_2$  in DMSO solution.  $\alpha\text{-Toc}^\bullet$  radical was prepared by the first-mixing of equal volumes of  $\alpha$ -TocH and  $\text{ArO}^\bullet$  solutions, and after 2 s the second-mixing of equal volumes of  $\alpha\text{-Toc}^\bullet$  solution and  $\text{PQQH}_2$  solution (reaction 3) was performed (see Figure 6A). The decay curves of the absorbance of  $\alpha\text{-Toc}^\bullet$  at 428 nm in DMSO are shown in Figure 6B. The baseline corrections were performed by using the value of  $\epsilon = 1120 \text{ M}^{-1} \text{ cm}^{-1}$  at 428 nm of  $\text{PQQH}_2$  in DMSO. Decay curves obtained by baseline correction are shown in Figure 6C, indicating that the decay rates increase with increasing concentrations of  $\text{PQQH}_2$ .

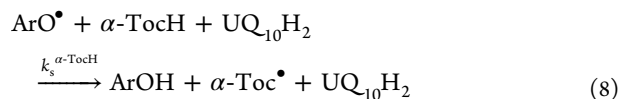
The  $k_{\text{obsd}}$  versus  $[\text{PQQH}_2]$  plot is also shown in Figure 5B.  $k_r$  values obtained for  $\text{UQ}_{10}\text{H}_2$  and  $\text{PQQH}_2$  are  $3.57 \times 10^4$  and  $1.08 \times 10^5 \text{ M}^{-1} \text{ s}^{-1}$ , respectively, as listed in Table 1. The rate constant ( $k_r$ ) of  $\text{PQQH}_2$  is 3.0 times larger than that of  $\text{UQ}_{10}\text{H}_2$ .  $k_r$  values obtained are very fast and about 2–3 orders of magnitude larger than those for  $k_s^{\alpha\text{-TocH}}$  (alone) (avg  $7.34 \times 10^2 \text{ M}^{-1} \text{ s}^{-1}$ ),  $k_s^{\text{UQ}_{10}\text{H}_2}$  (alone) (avg  $1.23 \times 10^3 \text{ M}^{-1} \text{ s}^{-1}$ ), and  $k_s^{\text{PQQH}_2}$  (alone) (avg  $2.52 \times 10^2 \text{ M}^{-1} \text{ s}^{-1}$ ).



**Figure 5.** (A) Time dependences of the absorbance of  $\alpha\text{-Toc}^\bullet$  radical at 428 nm in DMSO including six different concentrations of  $\text{UQ}_{10}\text{H}_2$  at  $25.0^\circ\text{C}$ . (B)  $k_{\text{obsd}}$  versus  $[\text{AOH}]$  ( $\text{AOH} = \text{UQ}_{10}\text{H}_2$  or  $\text{PQQH}_2$ ) plot.

**Measurements of the Aroxyl Radical-Scavenging Rates ( $k_s$ ) for Mixtures of  $\alpha$ -Tocopherol and Ubiquinol-10 in DMSO.** Measurements of the  $k_s^{\alpha\text{-TocH}}$  ( $+\text{UQ}_{10}\text{H}_2$ ) and  $k_s^{\text{UQ}_{10}\text{H}_2}$  ( $+\alpha\text{-TocH}$ ) values were performed for the solution including  $\alpha$ -TocH and  $\text{UQ}_{10}\text{H}_2$ , the terms " $k_s^{\alpha\text{-TocH}}$  ( $+\text{UQ}_{10}\text{H}_2$ )" and " $k_s^{\text{UQ}_{10}\text{H}_2}$  ( $+\alpha\text{-TocH}$ )" indicate the rate constants obtained in the solution including two components of AOHs. First, the  $k_s^{\alpha\text{-TocH}}$  ( $+\text{UQ}_{10}\text{H}_2$ ) value was measured by keeping  $[\text{UQ}_{10}\text{H}_2]$  constant ( $4.96 \times 10^{-4} \text{ M}$ ) and varying  $[\alpha\text{-TocH}]$  ( $0$  to  $1.89 \times 10^{-3} \text{ M}$ ). By mixing the solution of  $\text{ArO}^\bullet$  radical with the solution including  $\alpha$ -TocH and  $\text{UQ}_{10}\text{H}_2$ , absorption of the  $\text{ArO}^\bullet$  at 380 and 587 nm decreases rapidly, as shown in Figure 7A. Absorption of  $\alpha\text{-Toc}^\bullet$  at 428 nm was not observed at low  $[\alpha\text{-TocH}]$  ( $0$  to  $9.45 \times 10^{-4} \text{ M}$ ), but weak absorption appeared at high  $[\alpha\text{-TocH}]$  ( $(1.42\text{--}1.89) \times 10^{-3} \text{ M}$ ); see Figure 7B). By analysis of the decay curves of  $\text{ArO}^\bullet$  at 380 nm,  $k_{\text{obsd}}$  values were determined. Figure 7C shows the  $k_{\text{obsd}}$  versus  $[\alpha\text{-TocH}]$  plot.

If  $\alpha$ -TocH and  $\text{UQ}_{10}\text{H}_2$  coexist in solution, reactions 8 and 9 will occur competitively in solution, because the difference in the rate constants is less than two times, as listed in Table 1.



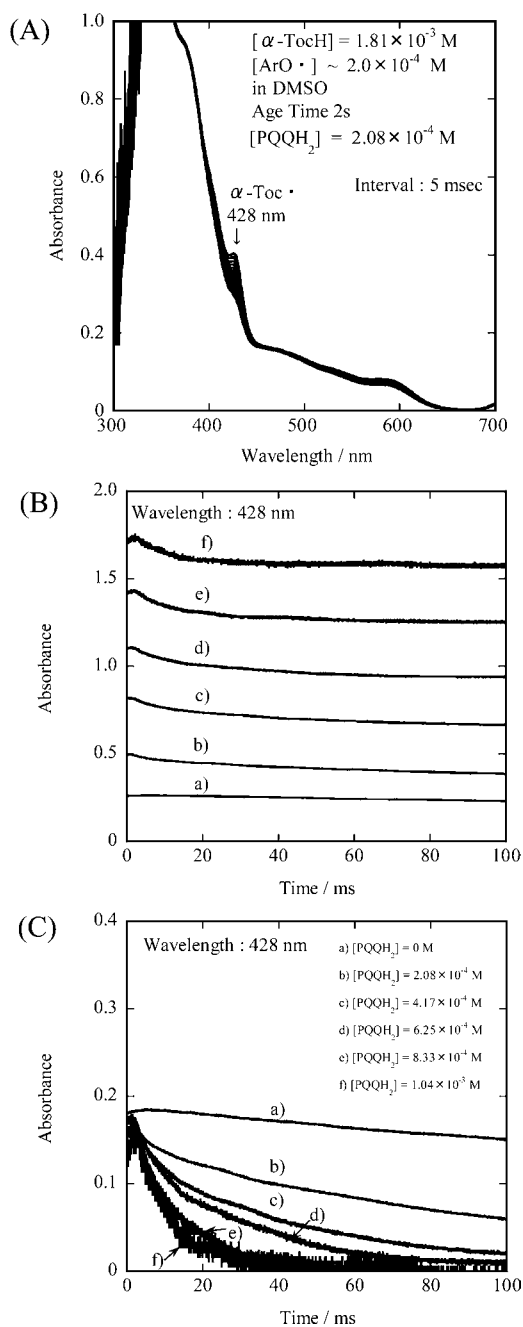
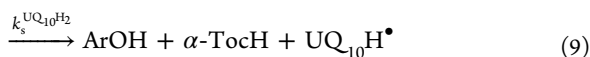
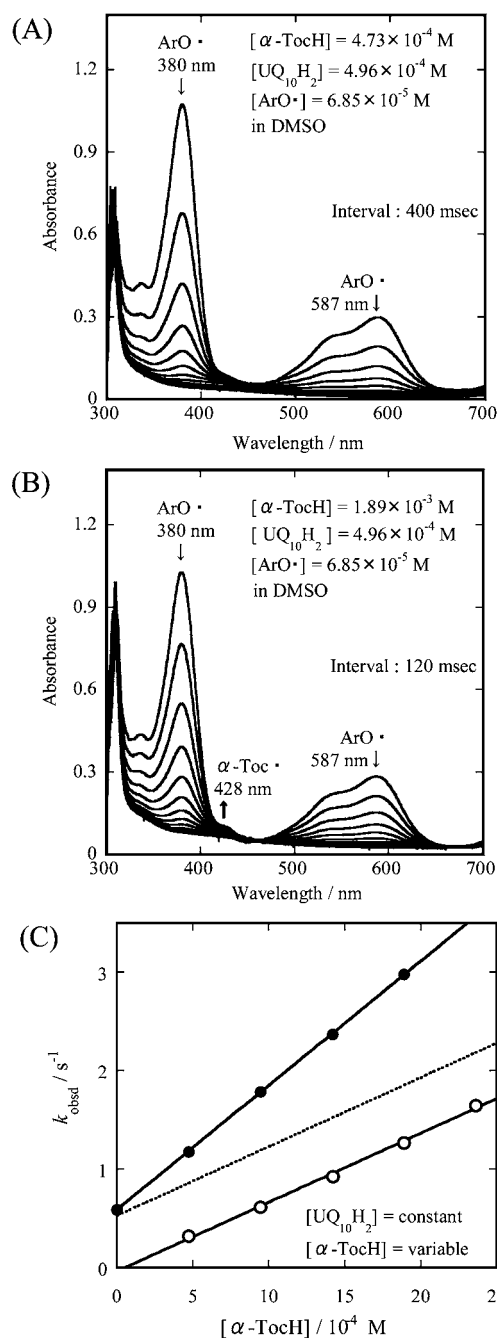


**Figure 6.** (A) Change in absorption spectrum (at 5 ms intervals) during reaction 3 of PQQH<sub>2</sub> and α-Toc• in DMSO at 25.0 °C. Initial concentration of [PQQH<sub>2</sub>] in cell C was 2.08 × 10<sup>-4</sup> M. Arrow indicates a decrease in absorbance of α-Toc•. (B) Absorbance decay of α-Toc• at 428 nm during reaction 3 in DMSO at 25.0 °C. (C) Baseline corrections for the absorption of PQQH<sub>2</sub> at 428 nm were performed.



In such a case, we can expect that the  $k_{\text{obsd}}$  value depends on eq 10, if the interaction between α-TocH and UQ<sub>10</sub>H<sub>2</sub> is negligible.

$$k_{\text{obsd}} = k_s^{\alpha\text{-TocH}}(\text{alone})[\alpha\text{-TocH}] + k_s^{\text{UQ}_{10}\text{H}_2}(\text{alone})[\text{UQ}_{10}\text{H}_2] \quad (10)$$

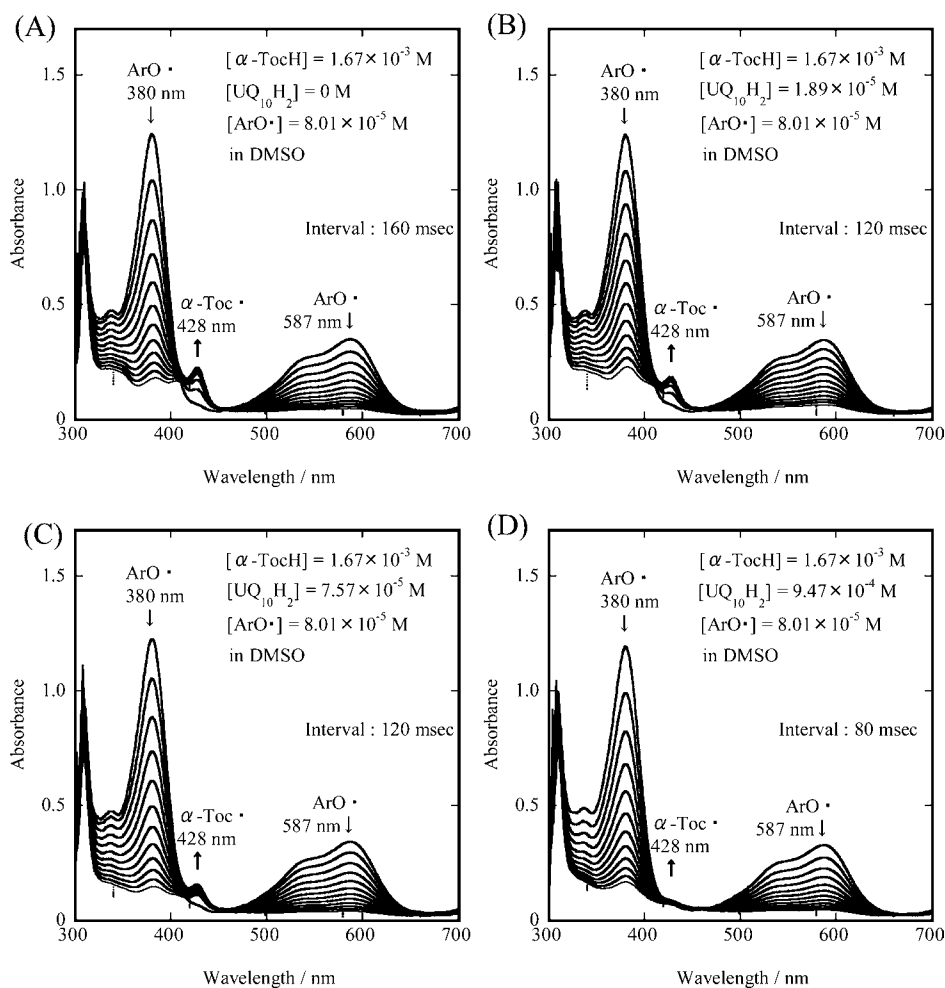


**Figure 7.** Change in electronic absorption spectrum of ArO• radical during reaction of ArO• with a mixture of α-TocH and UQ<sub>10</sub>H<sub>2</sub> in DMSO at 25.0 °C. [ArO•] = 6.85 × 10<sup>-5</sup> and [UQ<sub>10</sub>H<sub>2</sub>] = 4.96 × 10<sup>-4</sup> M. (A) [α-TocH] = 4.73 × 10<sup>-4</sup> M and (B) [α-TocH] = 1.89 × 10<sup>-3</sup> M. (C) Plots of  $k_{\text{obsd}}$  versus [α-TocH] for reactions of ArO• radical with (i) α-TocH only (○) and (ii) mixture of α-TocH and UQ<sub>10</sub>H<sub>2</sub> (●) (see Table 2A). Dotted line shows the plots for which any synergistic effect is absent between α-TocH and UQ<sub>10</sub>H<sub>2</sub>.

By substitution of  $k_s^{\alpha\text{-TocH}}$  (alone) and  $k_s^{\text{UQ}_{10}\text{H}_2}$  (alone) values and the value of [UQ<sub>10</sub>H<sub>2</sub>] (4.96 × 10<sup>-4</sup> M) used for measurement into eq 10,  $k_{\text{obsd}}$  was plotted against [α-TocH] (see a dotted line in Figure 7C). The result of the  $k_{\text{obsd}}$  versus [α-TocH] plot (open circle) obtained for the solution including only α-TocH is also shown in Figure 7C. As described above, measurement was performed, by keeping UQ<sub>10</sub>H<sub>2</sub> at a constant concentration and varying [α-TocH]. Consequently, the  $k_s^{\alpha\text{-TocH}}$

**Table 2.** Second-Order Rate Constants ( $k_s^{\text{AOH}}$  (+2nd AOH)) Obtained for Mixtures of Two Kinds of Antioxidants ((i)  $\alpha$ -TocH and UQ<sub>10</sub>H<sub>2</sub> and (ii)  $\alpha$ -TocH and PQQH<sub>2</sub>) and Ratios ( $k_s^{\text{AOH}}$  (+2nd AOH)/ $k_s^{\text{AOH}}$  (alone))

(A) Measurements Were Performed by Keeping [AOH] Constant and Varying [ $\alpha$ -TocH]				
antioxidant (AOH)	[AOH], M	[ $\alpha$ -TocH], M	$k_s^{\alpha\text{-TocH}} (+\text{AOH}),^a \text{ M}^{-1} \text{ s}^{-1}$	$k_s^{\alpha\text{-TocH}} (+\text{AOH})/k_s^{\alpha\text{-TocH}} (\text{alone})$
UQ <sub>10</sub> H <sub>2</sub>	$4.96 \times 10^{-4}$	$(0-1.89) \times 10^{-4}$	$(1.26 \pm 0.01) \times 10^3$	1.72
PQQH <sub>2</sub>	$3.71 \times 10^{-3}$	$(0-1.84) \times 10^{-3}$	$(8.26 \pm 0.40) \times 10^2$	1.13
(B) Measurements Were Performed by Keeping [ $\alpha$ -TocH] Constant and Varying [AOH]				
antioxidant (AOH)	[ $\alpha$ -TocH], M	[AOH], M	$k_s^{\text{AOH}} (+\alpha\text{-TocH}),^a \text{ M}^{-1} \text{ s}^{-1}$	$k_s^{\text{AOH}} (+\alpha\text{-TocH})/k_s^{\text{AOH}} (\text{alone})$
UQ <sub>10</sub> H <sub>2</sub>	$1.67 \times 10^{-3}$	$(0-3.55) \times 10^{-4}$ $(4.73-9.47) \times 10^{-4}$	$(3.08 \pm 0.08) \times 10^3$ $(6.33 \pm 2.19) \times 10^2$	2.50 0.515
PQQH <sub>2</sub>	$1.63 \times 10^{-3}$	$(0-3.06) \times 10^{-3}$	$(6.10 \pm 0.13) \times 10^2$	2.42

<sup>a</sup>Given as value  $\pm$  standard deviation (sd).**Figure 8.** Change in electronic absorption spectra of ArO<sup>•</sup> and  $\alpha$ -Toc<sup>•</sup> radicals during reaction of ArO<sup>•</sup> with mixture of  $\alpha$ -TocH and UQ<sub>10</sub>H<sub>2</sub> in DMSO at 25.0 °C. [ArO<sup>•</sup>] =  $8.01 \times 10^{-5}$  and [ $\alpha$ -TocH] =  $1.67 \times 10^{-3}$  M. Spectra were recorded at (A) 160 ms, (B) 120 ms, (C) 120 ms, and (D) 80 ms intervals. Absorption of  $\alpha$ -Toc<sup>•</sup> decreased with increasing concentrations of UQ<sub>10</sub>H<sub>2</sub>. (A) [UQ<sub>10</sub>H<sub>2</sub>] = 0 M, (B)  $1.89 \times 10^{-5}$  M, (C)  $7.57 \times 10^{-5}$  M, and (D)  $9.47 \times 10^{-4}$  M.

(+UQ<sub>10</sub>H<sub>2</sub>) value was determined from the gradient of the  $k_{\text{obsd}}$  versus [ $\alpha$ -TocH] plot (closed circle) in Figure 7C, using eq 11.

$$k_{\text{obsd}} = k_s^{\alpha\text{-TocH}}(+\text{UQ}_{10}\text{H}_2)[\alpha\text{-TocH}] + k_s^{\text{UQ}_{10}\text{H}_2}(\text{alone}) \quad (11)$$

As expected from the gradient in Figure 7C, the  $k_s^{\alpha\text{-TocH}}(+\text{UQ}_{10}\text{H}_2)$  value ( $1.26 \times 10^3 \text{ M}^{-1} \text{ s}^{-1}$ ) is 1.72 times larger than  $k_s^{\alpha\text{-TocH}}(\text{alone})$  ( $7.34 \times 10^2 \text{ M}^{-1} \text{ s}^{-1}$ ) obtained for the solution including only  $\alpha$ -TocH. A notable effect due to the coexistence

of  $\alpha$ -TocH and UQ<sub>10</sub>H<sub>2</sub> in solution was observed for the rate constant ( $k_s^{\alpha\text{-TocH}}(+\text{UQ}_{10}\text{H}_2)$ ).

As a notable effect of the coexistence of  $\alpha$ -TocH and UQ<sub>10</sub>H<sub>2</sub> was observed for the rate constants ( $k_s^{\alpha\text{-TocH}}(+\text{UQ}_{10}\text{H}_2)$ ), similar measurements were performed for the solutions including  $\alpha$ -TocH and UQ<sub>10</sub>H<sub>2</sub>, by keeping [ $\alpha$ -TocH] constant and varying [UQ<sub>10</sub>H<sub>2</sub>] (see Table 2B). As shown in Figure 8A–D, the absorption of  $\alpha$ -Toc<sup>•</sup> at 428 nm decreased with increasing the concentration of UQ<sub>10</sub>H<sub>2</sub>, suggesting that the  $\alpha$ -Toc<sup>•</sup> produced is regenerated quickly to  $\alpha$ -TocH by the

reaction with  $\text{UQ}_{10}\text{H}_2$  (reaction 3), because the regeneration rate constant ( $k_r = 3.57 \times 10^4 \text{ M}^{-1} \text{ s}^{-1}$ ) is very fast compared with the  $k_s^{\alpha\text{-TocH}} (+\text{UQ}_{10}\text{H}_2)$  value ( $1.26 \times 10^3 \text{ M}^{-1} \text{ s}^{-1}$ ).

As shown in Figure 3B, the  $k_{\text{obsd}}$  versus  $[\text{UQ}_{10}\text{H}_2]$  plot (closed circle) consists of two lines having different gradients. The analysis of the rate constant ( $k_s^{\text{UQ}_{10}\text{H}_2} (+\alpha\text{-TocH})$ ) was performed tentatively by using eq 12 similar to eq 11.

$$k_{\text{obsd}} = k_s^{\alpha\text{-TocH}}(\text{alone})[\alpha\text{-TocH}] + k_s^{\text{UQ}_{10}\text{H}_2} (+\alpha\text{-TocH}) [\text{UQ}_{10}\text{H}_2] \quad (12)$$

The  $k_s^{\text{UQ}_{10}\text{H}_2} (+\alpha\text{-TocH})$  values obtained at low and high  $[\text{UQ}_{10}\text{H}_2]$  ( $(0\text{--}3.55) \times 10^{-4}$  and  $(4.73\text{--}9.47) \times 10^{-4} \text{ M}$ ) are  $3.08 \times 10^3$  and  $6.33 \times 10^2 \text{ M}^{-1} \text{ s}^{-1}$ , respectively (see Table 2B). The  $k_s^{\text{UQ}_{10}\text{H}_2} (+\alpha\text{-TocH})$  values of the former and the latter are 2.50 and 0.515 times larger and smaller than the  $k_s^{\text{UQ}_{10}\text{H}_2}$  (alone) value, respectively.

**Measurements of the Aroxyl Radical-Scavenging Rates ( $k_2$ ) for Mixtures of  $\alpha$ -Tocopherol and PQQH<sub>2</sub> in DMSO.** Similar measurements (see Table 2A) were performed for the solution including  $\alpha$ -TocH and PQQH<sub>2</sub> by keeping  $[\text{PQQH}_2]$  constant and varying  $[\alpha\text{-TocH}]$ . The scavenging rate ( $k_{\text{obsd}}$ ) of  $\text{ArO}^\bullet$  was measured by following the decrease in absorbance at 587 nm of the  $\text{ArO}^\bullet$  radical (see Figure 9A).<sup>17</sup> The  $k_{\text{obsd}}$  versus  $[\alpha\text{-TocH}]$  plot is shown in Figure 9B. As performed for mixture of  $\alpha$ -TocH and  $\text{UQ}_{10}\text{H}_2$  (see eq 11), the  $k_s^{\alpha\text{-TocH}} (+\text{PQQH}_2)$  values were determined. The  $k_s^{\alpha\text{-TocH}} (+\text{PQQH}_2)$  values ( $8.26 \times 10^2 \text{ M}^{-1} \text{ s}^{-1}$ ) obtained under the coexistence of PQQH<sub>2</sub> are 1.13 times larger than the  $k_s^{\alpha\text{-TocH}}$  (alone) value (avg  $7.34 \times 10^2 \text{ M}^{-1} \text{ s}^{-1}$ ).

The  $k_s^{\text{PQQH}_2} (+\alpha\text{-TocH})$  value was measured by keeping  $[\alpha\text{-TocH}]$  constant ( $1.63 \times 10^{-3} \text{ M}$ ) and varying  $[\text{PQQH}_2]$  ( $(0\text{--}3.06) \times 10^{-3} \text{ M}$ ) (see Table 2B). As shown in Figure 10A–D, absorption of  $\alpha\text{-Toc}^\bullet$  at 428 nm decreased with increasing concentration of PQQH<sub>2</sub>, suggesting that the  $\alpha\text{-Toc}^\bullet$  produced is regenerated quickly to  $\alpha\text{-TocH}$  by reaction with PQQH<sub>2</sub> (reaction 3), because the regeneration rate constant ( $k_r$ ) ( $1.08 \times 10^5 \text{ M}^{-1} \text{ s}^{-1}$ ) is very fast compared with the  $k_s^{\alpha\text{-TocH}} (+\text{PQQH}_2)$  value ( $8.26 \times 10^2 \text{ M}^{-1} \text{ s}^{-1}$ ).

Figure 4C shows the  $k_{\text{obsd}}$  versus  $[\text{PQQH}_2]$  plot. From the gradient, the  $k_s^{\text{PQQH}_2} (+\alpha\text{-TocH})$  value ( $6.10 \times 10^2 \text{ M}^{-1} \text{ s}^{-1}$ ) was obtained. The value is 2.42 times larger than  $k_s^{\text{PQQH}_2}$  (alone) ( $2.52 \times 10^2 \text{ M}^{-1} \text{ s}^{-1}$ ). Large synergistic effect was observed under the coexistence of  $\alpha$ -TocH and PQQH<sub>2</sub>.

**Decrease in UV–Vis Absorption of  $\alpha$ -Tocopheroxyl Radical under the Coexistence of  $\alpha$ -Tocopherol and PQQH<sub>2</sub> (or Ubiquinol-10).** Upon reaction of  $\text{ArO}^\bullet$  radical with  $\alpha\text{-TocH}$ , absorption of  $\alpha\text{-Toc}^\bullet$  radical appears rapidly and decreases gradually, as shown in Figure 2D. The concentration of  $\alpha\text{-Toc}^\bullet$  radical ( $[\alpha\text{-Toc}^\bullet]$ ) produced by reaction with  $\text{ArO}^\bullet$  ( $[\text{ArO}^\bullet] = 6.85 \times 10^{-5} \text{ M}$ ) is similar to that of  $\text{ArO}^\bullet$ , if a high concentration of  $\alpha\text{-TocH}$  was used for the reaction, as described in a previous section and reported in a previous study.<sup>30</sup>

On the other hand, if  $\text{UQ}_{10}\text{H}_2$  coexists in the above solution, absorption of  $\alpha\text{-Toc}^\bullet$  radical at 428 nm decreases greatly with increasing  $[\text{UQ}_{10}\text{H}_2]$  and disappears at higher  $[\text{UQ}_{10}\text{H}_2]$ , as shown in Figure 8. The time dependence of  $[\alpha\text{-Toc}^\bullet]$  observed at  $\lambda_{\text{max}}$  (428 nm) is shown in Figure 11A, where  $[\alpha\text{-Toc}^\bullet]$  was calculated from the absorbance of  $\alpha\text{-Toc}^\bullet$ , using the relation (absorbance =  $\epsilon c l$ ,  $\epsilon = 3930 \text{ M}^{-1} \text{ cm}^{-1}$ ).<sup>30</sup> Figure 11B shows the  $[\alpha\text{-Toc}^\bullet]$  (at 1.5 s in Figure 11A) versus  $[\text{UQ}_{10}\text{H}_2]$  plot, indicating that the  $[\alpha\text{-Toc}^\bullet]$  at 1.5 s decreases rapidly with

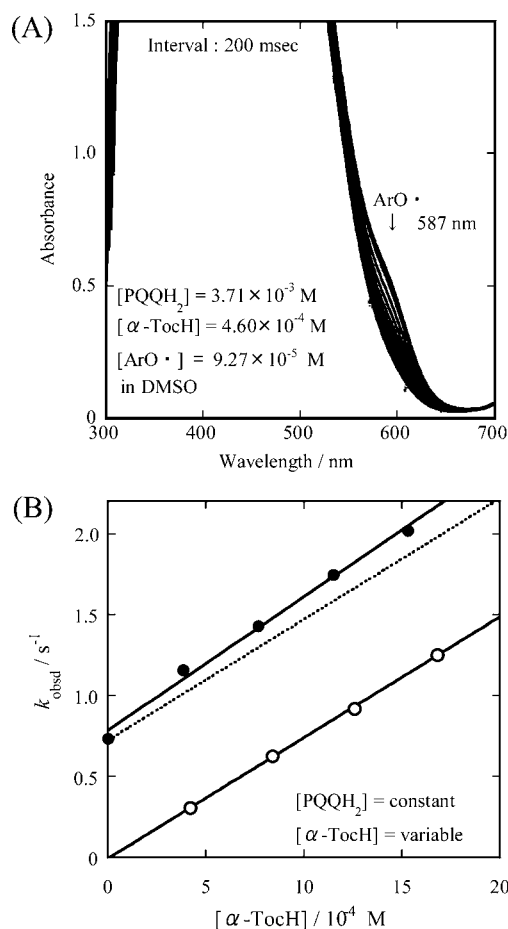


**Figure 9.** (A) Change in electronic absorption spectrum of  $\text{ArO}^\bullet$  radical during reaction of  $\text{ArO}^\bullet$  with a mixture of  $\alpha\text{-TocH}$  and  $\text{PQQH}_2$  in DMSO at 25.0 °C.  $[\text{ArO}^\bullet] = 9.27 \times 10^{-5}$ ,  $[\alpha\text{-TocH}] = 4.60 \times 10^{-4}$ , and  $[\text{PQQH}_2] = 3.71 \times 10^{-3} \text{ M}$ . (B) Plots of  $k_{\text{obsd}}$  versus  $[\alpha\text{-TocH}]$  for reaction of  $\text{ArO}^\bullet$  radical with (i)  $\alpha\text{-TocH}$  only (O) and (ii) mixture of  $\alpha\text{-TocH}$  and  $\text{PQQH}_2$  (●) (see Table 2A). Dotted line shows the plots for which any synergistic effect is absent between  $\alpha\text{-TocH}$  and  $\text{PQQH}_2$ .

increasing  $[\text{UQ}_{10}\text{H}_2]$ . As shown in Figure 11A, if  $[\text{UQ}_{10}\text{H}_2] \leq 1.89 \times 10^{-5} \text{ M}$  (plot c),  $\alpha\text{-Toc}^\bullet$  does not disappear at 10 s and remains in solution for a few minutes. However, if  $[\text{UQ}_{10}\text{H}_2] = 3.79 \times 10^{-5} \text{ M}$  (plot d), absorption of  $\alpha\text{-Toc}^\bullet$  disappears at  $\sim 7$  s. The result suggests that one molecule of  $\text{UQ}_{10}\text{H}_2$  quickly regenerates two molecules of  $\alpha\text{-Toc}^\bullet$  to two molecules of  $\alpha\text{-TocH}$ , because the initial  $[\alpha\text{-Toc}^\bullet]$  ( $= [\text{ArO}^\bullet]$ ) is  $8.01 \times 10^{-5} \text{ M}$  (see Figures 8 and 11). Two HO groups in  $\text{UQ}_{10}\text{H}_2$  molecule will contribute to the regeneration reaction of  $\alpha\text{-Toc}^\bullet$  radical. With increasing  $[\text{UQ}_{10}\text{H}_2]$  ((d)  $3.79 \times 10^{-5}$ , (e)  $5.68 \times 10^{-5}$ , (f)  $7.57 \times 10^{-5}$ , (g)  $1.18 \times 10^{-4} \text{ M}$ ), the time at which absorption of  $\alpha\text{-Toc}^\bullet$  disappears decreases in the order of  $\sim 7, 5, 4$ , and 3.5 s, respectively.

Similar measurements were performed for solutions including  $\alpha\text{-TocH}$  and  $\text{PQQH}_2$ . The time dependence of  $[\alpha\text{-Toc}^\bullet]$  observed at  $\lambda_{\text{max}}$  (428 nm) is shown in Figure 12A. Because the absorption of  $\text{PQQH}_2$  overlaps that of  $\alpha\text{-Toc}^\bullet$ , baseline correction was performed (see Figure 12B). As shown in Figure 12B,  $[\alpha\text{-Toc}^\bullet]$  decreases abruptly with increasing  $[\text{PQQH}_2]$ . The  $[\alpha\text{-Toc}^\bullet]$  (at 1.5 s in Figure 12B) versus  $[\text{PQQH}_2]$  plot is shown in Figure 12C, indicating that the  $[\alpha\text{-Toc}^\bullet]$  at 1.5 s decreases rapidly with increasing  $[\text{PQQH}_2]$ . As



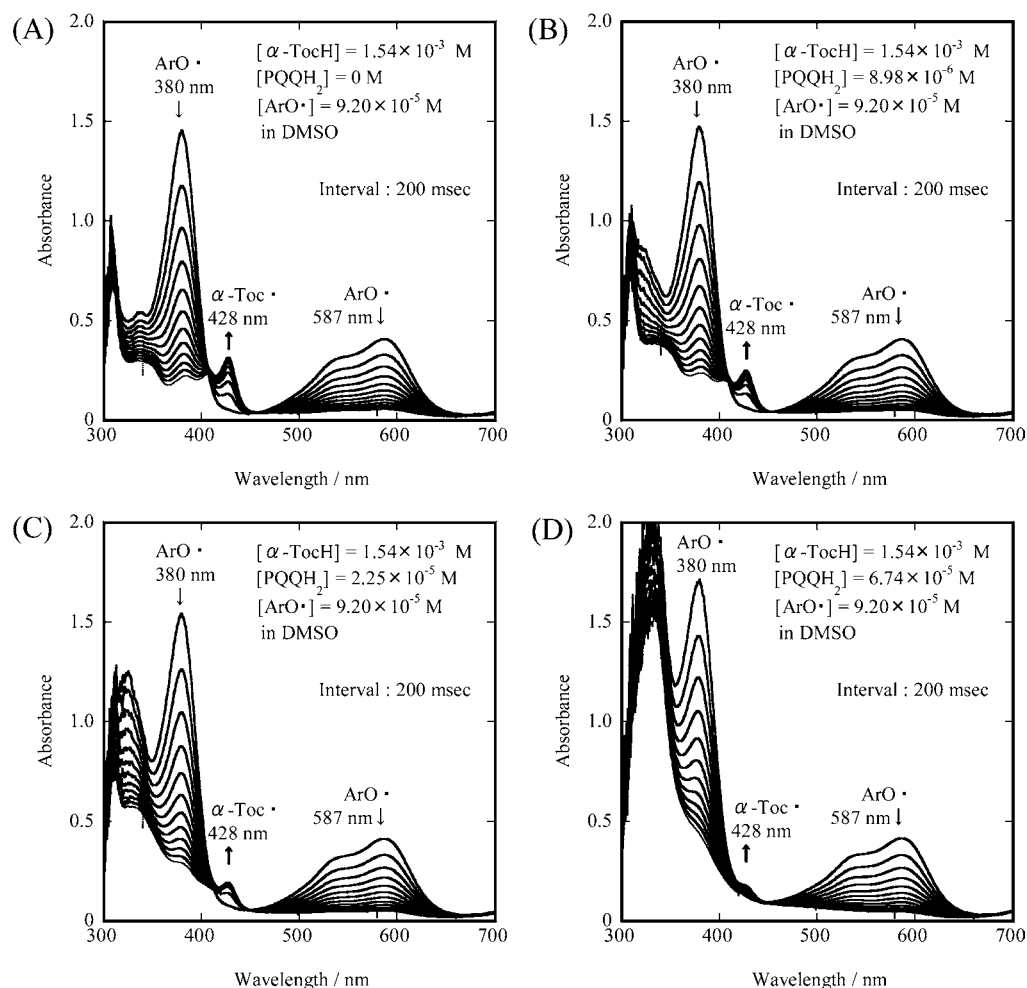
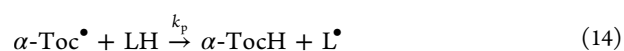
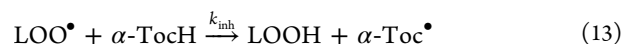


**Figure 10.** (A) Change in electronic absorption spectra of  $\text{ArO}^\bullet$  and  $\alpha\text{-Toc}^\bullet$  radicals during reaction of  $\text{ArO}^\bullet$  with a mixture of  $\alpha\text{-TocH}$  and  $\text{PQQH}_2$  in DMSO at 25.0 °C.  $[\text{ArO}^\bullet] = 9.20 \times 10^{-5}$  and  $[\alpha\text{-TocH}] = 1.54 \times 10^{-3}$  M. Spectra were recorded at 200 ms intervals. Absorption of  $\alpha\text{-Toc}^\bullet$  decreased with increasing concentrations of  $\text{PQQH}_2$ . (A)  $[\text{PQQH}_2] = 0$  M, (B)  $8.98 \times 10^{-6}$  M, (C)  $2.25 \times 10^{-5}$  M, and (D)  $6.74 \times 10^{-5}$  M.

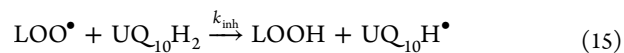
shown in Figure 12B, if  $[\text{PQQH}_2] = 4.49 \times 10^{-5}$  M (plot i), absorption of  $\alpha\text{-Toc}^\bullet$  completely disappears at  $\sim 9$  s. As observed for  $\text{UQ}_{10}\text{H}_2$ ,  $\text{PQQH}_2$  having two HO groups in a molecule may also quickly regenerate two molecules of  $\alpha\text{-Toc}^\bullet$  to two molecules of  $\alpha\text{-TocH}$ , because the initial  $[\alpha\text{-Toc}^\bullet]$  ( $= [\text{ArO}^\bullet]$ ) is  $9.20 \times 10^{-5}$  M (see Figures 10 and 12). Further, the result suggests that the contribution of NH group in  $\text{PQQH}_2$  to the regeneration reaction of  $\alpha\text{-Toc}^\bullet$  is negligible. With increasing  $[\text{PQQH}_2]$  ( $=$  (i)  $4.49 \times 10^{-5}$ , (j)  $6.74 \times 10^{-5}$ , (k)  $1.80 \times 10^{-4}$  M), the time at which absorption of  $\alpha\text{-Toc}^\bullet$  disappears decreases in the order of  $\sim 9, 5, 2$  s, respectively.

## DISCUSSION

**Comparison of Aroxyl Radical-Scavenging and  $\alpha$ -Tocopheroxyl-Regeneration Rates ( $k_s$  and  $k_r$ ) of  $\text{PQQH}_2$  with the Other Natural Antioxidants in DMSO Solution.**  $\alpha\text{-TocH}$  is well-known as one of the most important lipophilic antioxidants (AOHs) in foods and biological systems.<sup>32–35</sup> The antioxidant action of  $\alpha\text{-TocH}$  has been ascribed to the scavenging reaction of  $\text{LOO}^\bullet$ , producing the corresponding  $\alpha\text{-Toc}^\bullet$  radical (reaction 13).<sup>32</sup> On the other hand, if  $\alpha\text{-TocH}$  exists in biomembranes and edible oils,  $\alpha\text{-Toc}^\bullet$  radicals may react with unsaturated lipids (LHs) (reaction 14). Reaction 14 is known as a prooxidant reaction, which induces degradation of unsaturated lipids.<sup>36–39</sup>

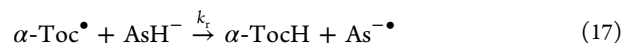


$\text{UQ}_{10}\text{H}_2$  is also well-known as a representative lipophilic AOH.<sup>40,41</sup>  $\text{UQ}_{10}\text{H}_2$  functions as an AOH by (i) scavenging  $\text{LOO}^\bullet$  (reaction 15) and (ii) regenerating  $\alpha\text{-Toc}^\bullet$  to  $\alpha\text{-TocH}$  (reaction 16),<sup>32,40,41</sup>



where  $\text{UQ}_{10}\text{H}^\bullet$  denotes a ubisemiquinone radical. The results of the kinetic studies for reactions 15 and 16 indicated that both reactions are important for the antioxidant actions of  $\text{UQ}_{10}\text{H}_2$ .<sup>29,42–44</sup>

On the other hand, Vit C (ascorbate monoanion,  $\text{AsH}^-$ ) is a representative water-soluble AOH. Hydrophilic  $\text{AsH}^-$  also enhances the antioxidant activity of  $\alpha\text{-TocH}$  by regenerating  $\alpha\text{-Toc}^\bullet$  to  $\alpha\text{-TocH}$  (reaction 17).<sup>45–47</sup>



where  $\text{As}^{\bullet-}$  is ascorbate free radical.

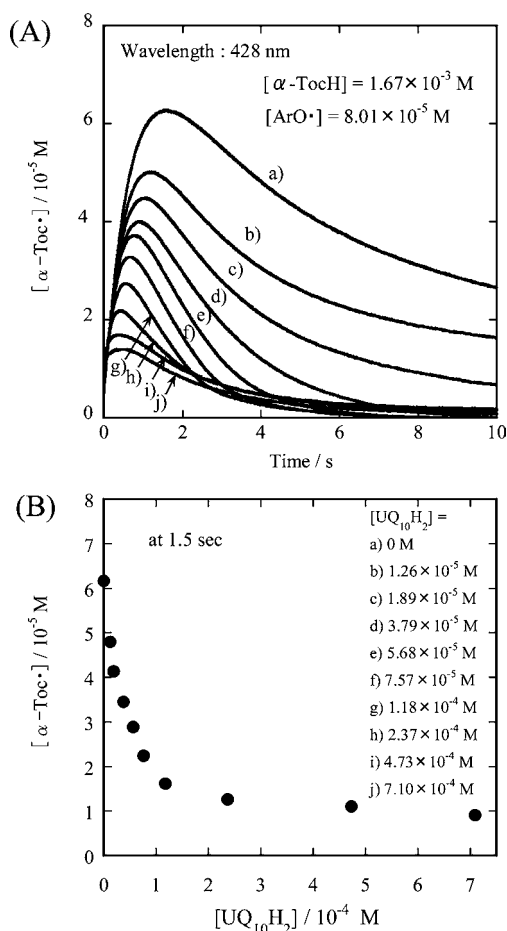


**Figure 11.** (A) Time dependences of the concentration of  $\alpha$ -Toc $\cdot$  radical  $[\alpha\text{-Toc}\cdot]$  (at 428 nm) in DMSO including 11 different concentrations of  $\text{UQ}_{10}\text{H}_2$  at 25.0 °C. (B)  $[\alpha\text{-Toc}\cdot]$  at 1.5 s in panel A versus  $[\text{UQ}_{10}\text{H}_2]$  plot.

In a previous study, we measured the  $k_s$  values for reaction of  $\text{ArO}\cdot$  radical with  $\text{PQQH}_2$  and water-soluble AOHs (Vit C, cysteine, glutathione, and UA) in 5.0 wt % Triton X-100 micellar solution (pH 7.4).<sup>17</sup> The  $k_s$  values decreased in the order of  $\text{PQQH}_2 > \text{Vit C} \gg \text{cysteine} > \text{UA} > \text{glutathione}$ . The  $k_s$  value of  $\text{PQQH}_2$  was 7.4 times larger than that of Vit C.

Furthermore, the  $k_Q$  values for reaction of  $^1\text{O}_2$  with  $\text{PQQH}_2$ ,  $\text{PQQNa}_2$ , and seven kinds of water- and lipid-soluble AOHs (Vit C, UA, EC, EGC,  $\alpha$ -TocH,  $\text{UQ}_{10}\text{H}_2$ , and  $\beta$ -Car) were measured in micellar solution (pH 7.4).<sup>27</sup> The  $k_Q$  values decreased in the order of  $\beta\text{-Car} > \text{PQQH}_2 > \alpha\text{-Toc} > \text{UA} > \text{UQ}_{10}\text{H}_2 > \text{Vit C} \approx \text{EGC} > \text{EC} \gg \text{PQQNa}_2$ . The  $^1\text{O}_2$ -quenching activity of  $\text{PQQH}_2$  was found to be 6.3, 2.2, 6.1, and 22 times larger than the corresponding ones of water-soluble AOHs (Vit C, UA, EGC, and EC). Further, the activity of  $\text{PQQH}_2$  was found to be 2.2 and 3.1 times larger than the corresponding ones of lipid-soluble AOHs ( $\alpha$ -Toc and  $\text{UQ}_{10}\text{H}_2$ ), respectively. On the other hand, the activity of  $\text{PQQH}_2$  is 6.4 times smaller than that of  $\beta$ -Car. The result suggests that  $\text{PQQH}_2$  may contribute to the protection of oxidative damage in biological systems, by quenching  $^1\text{O}_2$ .

In the present work,  $k_s$  value was measured for  $\text{PQQH}_2$  and seven AOHs in DMSO solution. As listed in Table 1, the  $k_s$  value of  $\text{PQQH}_2$  decreased in the order of eq 6. The  $k_s$  value of  $\text{PQQH}_2$  was greater than those of water-soluble AOHs (EGCG, EGC, EC, and CA). However, it was less than those

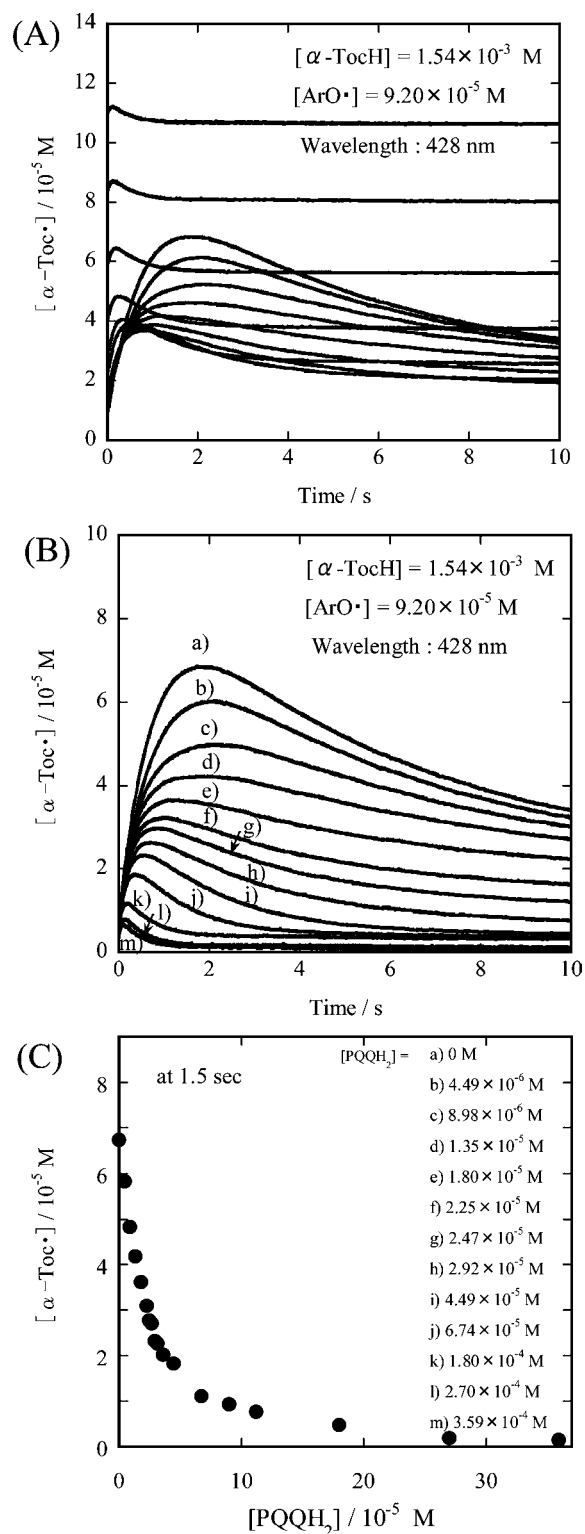


**Figure 12.** (A) Time dependences of the concentration of  $\alpha$ -Toc $\cdot$  radical  $[\alpha\text{-Toc}\cdot]$  (at 428 nm) in DMSO including 13 different concentrations of  $\text{PQQH}_2$  at 25.0 °C. (B) Baseline corrections for the absorption of  $\text{PQQH}_2$  in panel A were performed. (C)  $[\alpha\text{-Toc}\cdot]$  at 1.5 s in panel B versus  $[\text{PQQH}_2]$  plot.

of lipid-soluble AOHs ( $\alpha$ -TocH and  $\text{UQ}_{10}\text{H}_2$ ) in DMSO. Further, measurement of  $k_t$  value was performed for  $\text{PQQH}_2$  and  $\text{UQ}_{10}\text{H}_2$  in DMSO solution. The  $k_t$  value for  $\text{PQQH}_2$  was 3.0 times larger than that for  $\text{UQ}_{10}\text{H}_2$ , as listed in Table 1.

Measurements of the  $k_s$  and  $k_t$  values of Vit C (and  $\text{Na}^+\text{AsH}^-$ ) were tried in DMSO to compare with that of PQQH<sub>2</sub>. However, to our regret, we could not determine the  $k_s$  and  $k_t$  values, because of low solubility of Vit C (and  $\text{Na}^+\text{AsH}^-$ ) in DMSO.

As described above, the  $k_Q$  value of PQQH<sub>2</sub> was greater than those of  $\alpha$ -TocH and UQ<sub>10</sub>H<sub>2</sub> in micellar solution (pH 7.4). Similarly, the  $k_t$  value of PQQH<sub>2</sub> was greater than that of UQ<sub>10</sub>H<sub>2</sub> in DMSO. On the other hand, the  $k_s$  value of PQQH<sub>2</sub> was less than those of  $\alpha$ -TocH and UQ<sub>10</sub>H<sub>2</sub> in DMSO.

Catechins (EC, ECG, EGC, and EGCG) are catechol (or pyrogallol) derivatives. In previous works, detailed kinetic studies have been performed for the reaction of catechins with  $\text{ArO}^\bullet$  and 5,7-di-isopropyl-tocopheroxyl (5,7-di-iPr-Toc $^\bullet$ ) radicals in 5.0 wt % Triton X-100 solution.<sup>48,49</sup> The  $\text{ArO}^\bullet$  radical-scavenging and 5,7-di-iPr-Toc $^\bullet$  radical-regeneration rates ( $k_s$  and  $k_t$ ) of catechins were constant between pH = 4 and 6, and increased rapidly with increasing pH 6–10 in micellar solution. The increase of the  $k_s$  and  $k_t$  values was considered to be due to the deprotonation of HO group in catechins. PQQH<sub>2</sub> is also a catechol derivative. Consequently, we can expect that both  $k_s$  and  $k_t$  values of PQQH<sub>2</sub> increase with increasing pH value. It will be necessary to measure the pH dependence of the  $k_s$ ,  $k_t$ , and  $k_Q$  values of PQQH<sub>2</sub> in micellar solution in order to clarify the structure–activity relationship of the antioxidant activity of PQQH<sub>2</sub> in solution.

**Finding of Synergistic Effect on the Aroxyl Radical-Scavenging Rates ( $k_s$ ) under the Coexistence of  $\alpha$ -Tocopherol and PQQH<sub>2</sub> (or Ubiquinol-10).** The free radical-scavenging AOHs function not only individually but also synergistically with other AOHs. The most well-known interaction is the one between  $\alpha$ -TocH and Vit C.<sup>32,45–47</sup> Hydrophilic Vit C present in the aqueous phase efficiently reduces  $\alpha$ -Toc $^\bullet$  radical located within the membranes and lipoproteins to regenerate  $\alpha$ -TocH (reaction 17) and to inhibit the initiation of chain reaction induced by  $\alpha$ -Toc $^\bullet$  (that is the prooxidant effect of  $\alpha$ -TocH) (reaction 14). Similarly, lipophilic UQ<sub>10</sub>H<sub>2</sub> regenerates  $\alpha$ -TocH during lipid peroxidation in solution, liposomal membranes, low density protein, and mitochondrial membranes (reaction 16).<sup>29,40,41,43</sup>

It is well-known that various AOHs coexist in many foods and plants,<sup>33</sup> and biological systems.<sup>50–53</sup> However, the examples of measurement of free radical-scavenging rate under the coexistence of two AOHs are very limited, as far as we know.<sup>54</sup> Very recently, it has been found that the  $\text{ArO}^\bullet$  radical-scavenging rates ( $k_s$ ) increase notably under the coexistence of the above two AOHs ((i)  $\alpha$ -TocH and Vit C and (ii)  $\alpha$ -TocH and UQ<sub>10</sub>H<sub>2</sub>) in 2-propanol/water (5:1, v/v) solution.<sup>55</sup>

PQQ was found in many kinds of fruits and foods.<sup>3,13,56</sup> Furthermore, the existence of small amounts of free PQQ was found in eight human organs, plasma, and urine and in three rat organs.<sup>11</sup> The result suggests that PQQH<sub>2</sub> coexists with  $\alpha$ -TocH in many biological systems.

Therefore, in the present work, measurements of  $\text{ArO}^\bullet$  radical-scavenging rate ( $k_s^{\text{AOH}}$  (alone)) of AOHs ( $\alpha$ -TocH, PQQH<sub>2</sub>, and UQ<sub>10</sub>H<sub>2</sub>) were performed in DMSO solution. The  $k_s^{\text{AOH}}$  values were measured not only for each AOH, but also for mixtures of two kinds of AOHs ((i)  $\alpha$ -TocH and PQQH<sub>2</sub> and (ii)  $\alpha$ -TocH and UQ<sub>10</sub>H<sub>2</sub>). As described in the Results section, a notable synergistic effect was observed for the  $k_s^{\text{AOH}}$  values. For example, the  $k_s^{\alpha\text{-TocH}}$  (+UQ<sub>10</sub>H<sub>2</sub>) value ( $1.26 \times 10^3 \text{ M}^{-1} \text{ s}^{-1}$ ) obtained in solution including  $\alpha$ -TocH and

UQ<sub>10</sub>H<sub>2</sub> was 1.72 times larger than the  $k_s^{\alpha\text{-TocH}}$  (alone) value (avg  $7.34 \times 10^2 \text{ M}^{-1} \text{ s}^{-1}$ ) in solution including only  $\alpha$ -TocH (see Tables 1 and 2). The effect of the coexistence of  $\alpha$ -TocH and UQ<sub>10</sub>H<sub>2</sub> was more notable for the  $k_s^{\text{UQ}_{10}\text{H}_2}$  (+ $\alpha$ -TocH). Especially, at low concentration region of UQ<sub>10</sub>H<sub>2</sub> ( $(0\text{--}3.55) \times 10^{-4} \text{ M}$ ),  $k_s^{\text{UQ}_{10}\text{H}_2}$  (+ $\alpha$ -TocH) ( $3.08 \times 10^3 \text{ M}^{-1} \text{ s}^{-1}$ ) was 2.50 times larger than the  $k_s^{\text{UQ}_{10}\text{H}_2}$  (alone) (avg  $1.23 \times 10^3 \text{ M}^{-1} \text{ s}^{-1}$ ).

Furthermore, the  $k_s^{\alpha\text{-TocH}}$  (+PQQH<sub>2</sub>) ( $8.26 \times 10^2 \text{ M}^{-1} \text{ s}^{-1}$ ) was 1.13 times larger than the  $k_s^{\alpha\text{-TocH}}$  (alone) (avg  $7.34 \times 10^2 \text{ M}^{-1} \text{ s}^{-1}$ ; see Table 1). Similarly, the  $k_s^{\text{PQQH}_2}$  (+ $\alpha$ -TocH) ( $6.10 \times 10^2 \text{ M}^{-1} \text{ s}^{-1}$ ) was 2.42 times larger than the  $k_s^{\text{PQQH}_2}$  (alone) (avg  $2.52 \times 10^2 \text{ M}^{-1} \text{ s}^{-1}$ ).

As described above, notable increase of the  $\text{ArO}^\bullet$  radical-scavenging rate ( $k_s^{\text{AOH}}$ ) was observed for the AOHs under the coexistence of AOHs. However, the mechanism why the  $k_s^{\text{AOH}}$  values increase under the coexistence of two AOHs is not clear at present.<sup>55</sup>

#### UV–Vis Absorption of $\alpha$ -Tocopheroxyl Radical Disappears under the Coexistence of $\alpha$ -Tocopherol and PQQH<sub>2</sub> (or Ubiquinol-10): Suppression of Prooxidant Effect of $\alpha$ -Tocopherol.

As described above,  $\alpha$ -Toc $^\bullet$  is an important key radical, which appears in the process of the antioxidant and prooxidant actions of  $\alpha$ -TocH (see reactions 13–17). As described in the Results section, formation of  $\alpha$ -Toc $^\bullet$  radical was suppressed remarkably under the coexistence of  $\alpha$ -TocH and PQQH<sub>2</sub> (or UQ<sub>10</sub>H<sub>2</sub>). As shown in Figures 8 and 10–12, we could directly ascertain that  $\alpha$ -Toc $^\bullet$  radical produced by the reaction with  $\text{ArO}^\bullet$  radical immediately disappears through the regeneration reaction with PQQH<sub>2</sub> and UQ<sub>10</sub>H<sub>2</sub>, by observing the decrease of UV–vis absorption of  $\alpha$ -Toc $^\bullet$  radical. Furthermore, it has been clarified that PQQH<sub>2</sub> or UQ<sub>10</sub>H<sub>2</sub> having two OH groups within a molecule may rapidly regenerate two molecules of  $\alpha$ -Toc $^\bullet$  to two molecules of  $\alpha$ -TocH. In fact, the regeneration rate constants ( $k_t$ ) obtained for PQQH<sub>2</sub> and UQ<sub>10</sub>H<sub>2</sub> were very fast, as listed in Table 1. An example for such a direct observation of the disappearance of  $\alpha$ -Toc $^\bullet$  radical under the coexistence of  $\alpha$ -TocH and PQQH<sub>2</sub> (or UQ<sub>10</sub>H<sub>2</sub>) has not been reported, as far as we know.

As described above,  $\alpha$ -TocH, PQQH<sub>2</sub>, and UQ<sub>10</sub>H<sub>2</sub> coexist in foods and biological systems (such as plasma, blood, and various tissues).<sup>3,11,13,56</sup> Consequently, the above synergistic effect, that is, the increase of the free radical-scavenging rate and the suppression of the prooxidant reaction, may function in foods and biological systems.

## AUTHOR INFORMATION

### Corresponding Authors

\*(K.M.) Tel: 81-89-927-9588. Fax: 81-89-927-9590. E-mail: mukai-k@dpc.ehime-u.ac.jp,

\*(A.O.) E-mail: ouchiaya@dpc.ehime-u.ac.jp.

### Funding

This work was partly supported by a Grant-in-Aid for Challenging Exploratory Research (No. 24658123) from the Japan Society for the Promotion of Science.

### Notes

The authors declare no competing financial interest.

## REFERENCES

- (1) Duine, J. A.; Frank, J. J.; Jongejan, J. A. Glucose dehydrogenase from *Acinetobacter calcoaceticus*. A 'quinoprotein'. *FEBS Lett.* **1979**, *108*, 443–446.



- (2) Salisbury, S. A.; Forrrest, H. S.; Gruse, W. B. T.; Kennard, O. A novel coenzyme from bacterial primary alcohol dehydrogenases. *Nature* **1979**, *280*, 843–844.
- (3) Stites, T. E.; Mitchel, A. E.; Rucker, R. B. Physiological importance of quinoenzymes and o-quinone family of cofactors. *J. Nutr.* **2000**, *130*, 719–727.
- (4) Rucker, R.; Chowanadisai, W.; Nakano, M. Potential physiological importance of pyrroloquinoline quinone. *Altern. Med. Rev.* **2009**, *14*, 268–277.
- (5) Killgore, J.; Smidt, C.; Duich, L.; Romero-Chapman, N.; Tinker, D.; Reiser, K.; Melko, M.; Hyde, D.; Rucker, R. B. Nutritional importance of pyrroloquinoline quinone. *Science* **1989**, *245*, 850–852.
- (6) Bauerly, K. A.; Storms, D. H.; Harris, C. B.; Hajizadeh, S.; Sun, M. Y.; Cheung, C. P.; Satre, M. A.; Fascetti, A. J.; Tchapanian, E.; Rucker, R. B. Pyrroloquinoline quinone nutritional status alters lysine metabolism and modulates mitochondrial DNA content in the mouse and rat. *Biochim. Biophys. Acta* **2006**, *1760*, 1741–1748.
- (7) Chowanadisai, W.; Bauerly, K. A.; Tchapanian, E.; Wong, A.; Cortopassi, G. A.; Rucker, R. B. Pyrroloquinoline quinone stimulates mitochondrial biogenesis through cAMP response element-binding protein phosphorylation and increased PGC-1 $\alpha$  expression. *J. Biol. Chem.* **2010**, *285*, 142–52.
- (8) Yamaguchi, K.; Sasano, A.; Urakami, T.; Tsuji, T.; Kondo, K. Stimulation of nerve growth factor production by pyrroloquinoline quinone and its derivatives in vitro and in vivo. *Biosci., Biotechnol., Biochem.* **1993**, *57*, 1231–1233.
- (9) Liu, S.; Li, H.; Yang, J.; Peng, H.; Wu, K.; Liu, Y.; Yang, J. Enhanced rat sciatic nerve regeneration through silicon tubes filled with pyrroloquinoline quinone. *Microsurgery* **2005**, *25*, 329–337.
- (10) Hirakawa, A.; Shimizu, K.; Fukumitsu, H.; Furukawa, S. Pyrroloquinoline quinone attenuates iNOS gene expression in the injured spinal cord. *Biochem. Biophys. Res. Commun.* **2009**, *378*, 308–312.
- (11) Kumazawa, T.; Seno, H.; Urakami, T.; Matsumoto, T.; Suzuki, O. Trace levels of pyrroloquinoline quinone in human and rat samples detected by gas chromatography/mass spectroscopy. *Biochim. Biophys. Acta* **1992**, *1156*, 62–66.
- (12) Mitchell, A. E.; Johnes, A. D.; Mercer, R. S.; Rucker, R. B. Characterization of pyrroloquinoline quinone amino acid derivatives by electrospray ionization mass spectrometry and detection in human milk. *Anal. Biochem.* **1999**, *269*, 317–325.
- (13) Kumazawa, T.; Sato, K.; Seno, H.; Ishii, A.; Suzuki, O. Levels of pyrroloquinoline quinone in various foods. *Biochem. J.* **1995**, *307*, 331–333.
- (14) Noji, N.; Nakamura, T.; Kitahata, N.; Taguchi, K.; Kudo, T.; Yoshida, S.; Tsujimoto, M.; Sugiyama, T.; Asami, T. Simple and sensitive method for pyrroloquinoline quinone (PQQ) analysis in various foods using liquid chromatography/electrospray-ionization tandem mass spectrometry. *J. Agric. Food Chem.* **2007**, *55*, 7258–7263.
- (15) Miyauchi, K.; Urakami, T.; Abeta, H.; Shi, H.; Noguchi, N.; Niki, E. Action of pyrroloquinolinequinol as an antioxidant against lipid peroxidation in solution. *Antioxid. Redox Signaling* **1999**, *1*, 547–554.
- (16) He, K.; Nukada, H.; Urakami, T.; Murphy, M. P. Antioxidant and pro-oxidant properties of pyrroloquinoline quinone (PQQ): implications for its function in biological systems. *Biochem. Pharmacol.* **2003**, *65*, 67–74.
- (17) Ouchi, A.; Nakano, M.; Nagaoka, S.; Mukai, K. Kinetic study of the antioxidant activity of pyrroloquinolinequinol (PQQH<sub>2</sub>, a reduced form of pyrroloquinolinequinone) in micellar solution. *J. Agric. Food Chem.* **2009**, *57*, 450–456.
- (18) Hara, H.; Hiramatsu, H.; Adachi, T. Pyrroloquinoline quinone is a potent neuroprotective nutrient against 6-hydroxydopamine-induced neurotoxicity. *Neurochem. Res.* **2007**, *32*, 489–495.
- (19) Nunome, K.; Miyazaki, S.; Nakano, M.; Iguchi-Ariga, S.; Ariga, H. Pyrroloquinoline quinone prevents oxidative stress-induced neuronal death probably through changes in oxidative status of DJ-1. *Biol. Pharm. Bull.* **2008**, *31*, 1321–1326.
- (20) Zhu, B.-q.; Simonis, U.; Cecchini, G.; Zhou, H.-Z.; Li, L.; Teerlink, J. R.; Karliner, J. S. Comparison of pyrroloquinoline quinone and/or metoprolol on myocardial infarct size and mitochondrial damage in a rat model of ischemia/reperfusion injury. *J. Cardiovasc. Pharmacol. Ther.* **2006**, *11*, 119–128.
- (21) Zhang, Y.; Feustel, P. J.; Kimelberg, H. K. Neuroprotection by pyrroloquinoline quinone (PQQ) in reversible middle cerebral artery occlusion in the adult rat. *Brain Res.* **2006**, *1094*, 200–206.
- (22) Ohwada, K.; Takeda, H.; Yamazaki, M.; Isogaki, H.; Nakano, M.; Shimomura, M.; Fukui, K.; Urano, S. Pyrroloquinoline quinone (PQQ) prevents cognitive deficit caused by oxidative stress in rats. *J. Clin. Biochem. Nutr.* **2008**, *42*, 29–34.
- (23) Takatsu, H.; Owada, K.; Abe, K.; Nakano, M.; Urano, S. Effect of vitamin E on learning and memory deficit in aged rats. *J. Nutr. Sci. Vitaminol.* **2009**, *55*, 389–393.
- (24) Mukai, K.; Kageyama, Y.; Ishida, T.; Fukuda, K. Synthesis and kinetic study of antioxidant activity of new tocopherol (vitamin E) compounds. *J. Org. Chem.* **1989**, *54*, 552–556.
- (25) Mukai, K.; Daifuku, K.; Okabe, K.; Tanigaki, T.; Inoue, K. Structure–activity relationship in the quenching reaction of singlet oxygen by tocopherol (vitamin E) derivatives and related phenols. Finding of linear correlation between the rates of quenching of singlet oxygen and scavenging of peroxy and phenoxy radicals in solution. *J. Org. Chem.* **1991**, *56*, 4188–4192.
- (26) Mukai, K.; Tokunaga, A.; Itoh, S.; Kanesaki, Y.; Ohara, K.; Nagaoka, S.; Abe, K. Structure–activity relationship of the free-radical-scavenging reaction by vitamin E ( $\alpha$ -,  $\beta$ -,  $\gamma$ -,  $\delta$ -tocopherols) and ubiquinol-10: pH dependence of the reaction rates. *J. Phys. Chem. B* **2007**, *111*, 652–662.
- (27) Mukai, K.; Ouchi, A.; Nakano, M. Kinetic study of the quenching reaction of singlet oxygen by pyrroloquinolinequinol (PQQH<sub>2</sub>, a reduced form of pyrroloquinolinequinone) in micellar solution. *J. Agric. Food Chem.* **2011**, *59*, 1705–1712.
- (28) Rieker, A.; Scheffler, K. Die beteiligung von phenylresten an der aroxylmesomerie. *Liebigs Ann. Chem.* **1965**, *689*, 78–92.
- (29) Ouchi, A.; Nagaoka, S.; Mukai, K. Tunneling effect in regeneration reaction of vitamin E by ubiquinol. *J. Phys. Chem. B* **2010**, *114*, 6601–6607.
- (30) Mukai, K.; Ouchi, A.; Mitarai, A.; Ohara, K.; Matsuoka, C. Formation and decay dynamics of vitamin E radical in the antioxidant reaction of vitamin E. *Bull. Chem. Soc. Jpn.* **2009**, *82*, 494–503.
- (31) Parker, A. W.; Hester, R. E.; Phillips, D.; Umapathy, S. Time-resolved resonance raman spectroscopic investigations of the photochemistry of ubiquinone. *J. Chem. Soc., Faraday Trans.* **1992**, *88*, 2649–2653.
- (32) Niki, E. Assessment of antioxidant capacity in vitro and in vivo. *Free Radical Biol. Med.* **2010**, *49*, 503–515.
- (33) Finley, J. W.; Kong, A.-N.; Hintze, K. J.; Jeffery, E. H.; Ji, L. L.; Lei, X. G. Antioxidants in foods: State of the science important to the food industry. *J. Agric. Food Chem.* **2011**, *59*, 6837–6846.
- (34) Esterbauer, H.; Dieber-Rotheneder, M.; Striegl, G.; Waeg, G. Role of vitamin E in preventing the oxidation of low-density lipoprotein. *Am. J. Clin. Nutr.* **1991**, *53*, 314S–321S.
- (35) Neuzil, J.; Thomas, S. R.; Stocker, R. Requirement for, promotion, or inhibition by  $\alpha$ -tocopherol of radical induced initiation of plasma lipoprotein lipid peroxidation. *Free Radical Biol. Med.* **1997**, *22*, 57–71.
- (36) Terao, J.; Matsushita, S. The peroxidizing effect of  $\alpha$ -tocopherol on autooxidation of methyl linoleate in bulk phase. *Lipids* **1986**, *21*, 255–260.
- (37) Bowry, V. W.; Stocker, R. Tocopherol-mediated peroxidation. The prooxidant effect of vitamin E on the radical-initiated oxidation of human low-density lipoprotein. *J. Am. Chem. Soc.* **1993**, *115*, 6029–6044.
- (38) Mukai, K.; Noborio, S.; Nagaoka, S. Why is the order reversed? Peroxyl-scavenging activity and fats-and-oils protecting activity of vitamin E. *Int. J. Chem. Kinet.* **2005**, *37*, 605–610.
- (39) Ouchi, A.; Ishikura, M.; Konishi, K.; Nagaoka, S.; Mukai, K. Kinetic study of the prooxidant effect of  $\alpha$ -tocopherol. Hydrogen



abstraction from lipids by  $\alpha$ -tocopheroxyl radical. *Lipids* **2009**, *44*, 935–943.

(40) Ernster, L.; Dallner, G. Biochemical, physiological and medical aspects of ubiquinone function. *Biochim. Biophys. Acta* **1995**, *1271*, 195–204.

(41) *Coenzyme Q: Molecular mechanisms in health and disease*; Kagan, V. E., Quinn, P. J., Eds.; CRC Press: Boca Raton, FL, 2001.

(42) Naumov, V. V.; Khrapova, N. G. Study of the interaction of ubiquinone and ubiquinol with peroxide radicals by the chemiluminescent method. *Biophysics (Engl. Transl. Biofizika)* **1983**, *28*, 774–780.

(43) Mukai, K.; Kikuchi, S.; Urano, S. Stopped-flow kinetic study of the regeneration reaction of tocopheroxyl radical by reduced ubiquinone-10 in solution. *Biochim. Biophys. Acta* **1990**, *1035*, 77–82.

(44) Barclay, L. R. C.; Vinqvist, M. R.; Mukai, K.; Itoh, S.; Morimoto, H. Chain-breaking phenolic antioxidants: Steric and electronic effects in polyalkylchromanols, tocopherol analogs, hydroquinones, and superior antioxidants of the polyalkylbenzochromanol and naphthofuran class. *J. Org. Chem.* **1993**, *58*, 7416–7420.

(45) Packer, J. E.; Slater, T. F.; Willson, R. L. Direct observation of a free radical interaction between vitamin E and vitamin C. *Nature* **1979**, *278*, 737–738.

(46) Mukai, K.; Nishimura, M.; Kikuchi, S. Stopped-flow investigation of the reaction of vitamin C with tocopheroxyl radical in aqueous Triton X-100 micellar solutions. *J. Biol. Chem.* **1991**, *266*, 274–278.

(47) Bisby, R. H.; Parker, A. W. Reaction of ascorbate with the  $\alpha$ -tocopheroxyl radical in micellar and bilayer membrane systems. *Arch. Biochem. Biophys.* **1995**, *317*, 170–178.

(48) Mitani, S.; Ouchi, A.; Watanabe, E.; Kanesaki, Y.; Nagaoka, S.; Mukai, K. Stopped-flow kinetic study of the aroxyl radical-scavenging action of catechins and vitamin C in ethanol and micellar solutions. *J. Agric. Food Chem.* **2008**, *56*, 4406–4417.

(49) Mukai, K.; Mitani, S.; Ohara, K.; Nagaoka, S. Structure-activity relationship of the tocopherol-regeneration reaction by catechins. *Free Radical Biol. Med.* **2005**, *38*, 1243–1256.

(50) Podda, M.; Weber, C.; Traber, M. G.; Packer, L. Simultaneous determination of tissue tocopherols, tocotrienols, ubiquinols, and ubiquinones. *J. Lipid Res.* **1996**, *37*, 893–901.

(51) Lass, A.; Foster, M. J.; Sohal, R. S. Effects of coenzyme Q<sub>10</sub> and  $\alpha$ -tocopherol administration on their tissue levels in the mouse: Elevation of mitochondrial  $\alpha$ -tocopherol by coenzyme Q<sub>10</sub>. *Free Radical Biol. Med.* **1999**, *26*, 1375–1382.

(52) Colome, C.; Artuch, R.; Vilaseca, M.-A.; Sierra, C.; Brandi, N.; Lambruschini, N.; Cambra, F. J.; Campistol, J. Lipophilic antioxidants in patients with phenylketonuria. *Am. J. Clin. Nutr.* **2003**, *77*, 185–188.

(53) Homma, Y.; Kondo, Y.; Kaneko, M.; Kitamura, T.; Nyu, W. T.; Yanagisawa, M.; Yamamoto, Y.; Kakizoe, T. Promotion of carcinogenesis and oxidative stress by dietary cholesterol in rat prostate. *Carcinogenesis* **2004**, *25*, 1011–1014.

(54) Niki, E.; Saito, T.; Kawakami, A.; Kamiya, Y. Inhibition of oxidation of methyl linoleate in solution by vitamin E and vitamin C. *J. Biol. Chem.* **1984**, *259*, 4177–4128.

(55) Mukai, K.; Ouchi, A.; Nakaya, S.; Nagaoka, S. Aroxyl-radical-scavenging rate increases remarkably under the coexistence of  $\alpha$ -tocopherol and ubiquinol-10 (or vitamin C): Finding of synergistic effect on the reaction rate. *J. Phys. Chem. B* **2013**, *117*, 8378–8391.

(56) Van der Meer, R. A.; Groen, B. W.; van Kleef, M. A. G.; Frank, J.; Jongejan, J. A.; Duine, J. A. Isolation, preparation, and assay of pyrroloquinoline quinone. *Methods Enzymol.* **1990**, *188*, 260–283.